ESA Climate Change Initiative (CCI)

Sea Level Budget Closure (SLBC_cci)

Sea Level Budget Closure Assessment Report
ESA_SLBC_cci_D3.3

(Version 1.2, issued 24 November 2019)

SLBC Assessment Report 3 based on version 2 data

Prime & Science Lead: Martin Horwath
Technische Universität Dresden (TUDr)
Martin.Horwath@tu-dresden.de

Technical Officer: Jérôme Benveniste
ESA ESRIN, Frascati, Italy
Jerome.Benveniste@esa.int

Contract No.: 4000 11 9910/17/I-NB

Consortium: Technische Universität Dresden (TUDr)
Laboratoire d'Etudes en Géophysique et Océanographie Spatiales (LEGOS)
Universität Bremen (UB)
Universität Zürich (UZH)
University of Leeds (UoL)
Goethe-Universität Frankfurt (GUF)
Danmarks Tekniske Universitet, DTU Space, Geodynamics (DTU-GDK)
Danmarks Tekniske Universitet, DTU Space, Geodesy (DTU-GEK)
Nansen Environmental and Remote Sensing Center (NERSC)
University of Reading (UoR)
Mercator Ocean, Toulouse (MerO)

To be cited as:

Horwath, M.; Novotny, K.; Cazenave, A.; Palanisamy, H.; Marzeion, B.; Paul, F.; Döll, P.; Cáceres, D.; Hogg, A.; Otosaka, I.; Shepherd, A.; Forsberg, R.; Barletta, V.R.; Andersen, O.B.; Rose, S.K.; H.; Johannessen, J.; Raj, R.P.; Gutknecht, B.D.; Merchant, Ch.J.; MacIntosh, C.R.; von Schuckmann, K.: *ESA Climate Change Initiative (CCI) Sea Level Budget Closure (SLBC_cci). SLBC Assessment Report 3 based on version 2 data (D3.3). Version 1.2, 24 November 2019.*

Signatures page

Prepared by	Kristin Novotny Project Manager, TUDr Martin Horwath Science Leader, TUDr Anny Cazenave, Hindumathi Palanisamy, LEGOS; Ben Marzeion, UB; Frank Paul, UZH; Petra Döll, Denise Cáceres, GUF; Anna Hogg, Inés Otosaka, Andrew Shepherd, UoL; Valentina Barletta, Rene Forsberg, DTU-GDK; Ole B. Andersen, Stine K. Rose, DTU-GEK; Johnny Johannessen, Roshin P. Raj, NERSC; Benjamin D. Gutknecht, TUDr; Christopher John Merchant, Claire Rachel MacIntosh, UoR; Karina von Schuckmann, MerO	Date: 2019-11-24 K. N
Checked by	Martin Horwath Science Leader, TUDr	Date: 2019-11-24 Martin Horwath
Approved by	Jérôme Benveniste Technical Officer, ESA	Date:

Change Log

Issue	Author, Org.	Affected Section	Reason/Description	Status
1.0	M. Horwath / TUDr	All	Document Creation	Released to ESA 2019-10-28
1.1	M. Horwath / TUDr	All	Document revision after review by ESA	Released to ESA 2019-11-15
1.2	M. Horwath / TUDr	All	Document revision after review by ESA	Released to ESA 2019-11-24

Distribution List

Organization	Consortium Member
TUDr	Martin Horwath
LEGOS	Anny Cazenave
UB	Ben Marzeion
UZH	Frank Paul
UoL	Andrew Shepherd, Anna Hogg
DTU- GDK	Rene Forsberg
GUF	Petra Döll
NERSC	Johnny Johannessen
DTU-GEK	Ole B. Andersen
UoR	Christopher Merchant
MerO	Karina von Schuckmann
ESA	Jérôme Benveniste Marco Restano Américo Ambrózio

Table of Contents

Acronyms and Abbreviations

Acronym	Explanation
AIS	Antarctic Ice Sheet
ALES	Adaptive Leading Edge Subwaveform
Argo	global array of temperature/salinity profiling floats
CCI, cci	Climate Change Initiative (initiated by ESA)
C-GLORS	CMCC Global Ocean Reanalysis System
CMC	Continental Mass Change
CMCC	Centro Euro-Mediterraneo sui Cambiamenti Climatici (Euro-Mediterranean Center on Climate Change)
CRU	Climatic Research Unit (University of East Anglia, Norwich, UK)
CRU TS	CRU Timeseries (grids of observed climate)
CSR	Center for Space Research (University of Texas at Austin)
CTD	conductivity, temperature, and depth
DTU	Danmarks Tekniske Universitet
DTU-GDK	DTU, Geodynamics Group
EN4	version 4 of the Met Office Hadley Centre ‘‘EN’’ series of data sets of global quality controlled ocean temperature and salinity profiles
ENSO	El Niño-Southern Oscillation
ERS-1/2	European Remote Sensing Satellite -1/2
ESA	European Space Agency
GAA, GAB, GAC, GAD	Names of data products related to GRACE atmospheric and oceanic background models (refer to section 3.2.2)
GFZ	GeoForschungsZentrum Potsdam
GIA	Glacial Isostatic Adjustment
GIS	Greenland Ice Sheet
GMB	Gravimetric Mass Balance / GRACE Mass Balance
GMSL	Global Mean Sea Level
GPCC	Global Precipitation Climatology Centre
GRACE	Gravity Recovery and Climate Experiment
GSFC	Goddard Space Flight Center
Gt	Gigatons
GUF	Goethe University Frankfurt
ICE-5G	models of postglacial relative sea-level history
ICESat	Ice, Cloud, and land Elevation Satellite, part of NASA's Earth Observing System
IPRC	International Pacific Research Center
ITSG	Institute of Geodesy, Theoretical Geodesy and Satellite Geodesy (TU Graz)
JAMSTEC	Japan Agency for Marine-earth Science and Technology
JPL	Jet Propulsion Laboratory
LEGOS	Laboratoire d’Etudes en Géophysique et Océanographie Spatiales
LRM	Low Resolution Mode

LWS	Land Water Storage
NERSC	Nansen Environmental and Remote Sensing Center
NOAA	National Oceanic and Atmospheric Administration
OGGM	Open Global Glacier Model
OMC	Ocean Mass Change
RGI	Randolph Glacier Inventory
RL05, RL06	(GRACE) solution Release 05/06
RMS	Root Mean Square
RSS	Root Square Sum
SCRIPPS	Scripps Institution of Oceanography (University of California)
SH	spherical harmonic
SL_cci	ESA CCI_Sea Level Project
SLBC	Sea Level Budget Closure
SLE	Sea Level Equivalent
SMOS	Soil Moisture and Ocean Salinity mission
SSH	Sea Surface Height
SSLA	Steric Sea Level Anomaly
STD	Standard Deviation
T&S	Temperature and Salinity
TOPAZ	(Towards) an Operational Prediction system for the North Atlantic European coastal Zones
TOPEX	TOPography EXperiment, part of the TOPEX/Poseidon satellite (joint radar altimetry project, NASA and CNES)
TU	Technische Universität / Technical University
TWS	Total Water Storage
UB	University of Bremen
UK	United Kingdom
UoL	University of Leeds
UoR	University of Reading
UZH	University of Zurich
v0, v1, v2	version 0, version 1, version 2 data set within SLBC_cci project
VM	model of the radial viscoelastic structure of the Earth (used fo ICE-5G)
WCRP	World Climate Research Programme
WFDEI	Watch Forcing Data based on ERA-Interim reanalysis
WGHM	Water GAP Global Hydrology Model
WGMS	World Glacier Monitoring Service
WP	Work Package
XBT	Expendable Bathythermograph
XCTD	Expendable Conductivity/Temperature and Depth

1 Introduction

1.1 Purpose and Scope

This document discusses the results of the sea level budget closure assessment at the final stage of the ESA CCI Sea Level Budget Closure (SLBC_cci) project. Comparisons and results are based on version 2 (v2) data as they are described in detail in the SLBC_cci Product Description Document D2.4.2 (Horwath et al. 2019), or are indicated individually otherwise. v2 data and products have been developed and gathered during the WP2x3 phase of the SLBC_cci project. They were improved over version 1 (v1). The results were discussed within the entire consortium during project meetings, at monthly telecons and in numerous bilateral discussions.

Changes and adaptations in datasets from contributing WPs lead to several changes and improvements as follows:

- Longer time-series (to end of 2016 vs 2014/2015 in v0/v1)
- Uncertainty assessments improved and updated to refer to the differences w.r.t. the reference interval 01/2006--12/2015
- Ocean Mass Change (OMC) improved by updated methodology (Horwath et al. 2019) and use of new GRACE releases with reduced noise (Groh et al. 2019); GRACE-based continental mass change (CMC) included.
- OGGM Glacier model updated, uncertainty assessment uptdated.
- GMB for GIS updated;
- Radar- and lidar altimetry results for GIS combined with peripheral glaciers assessment from OGGM to be consistent with GMB
- GMB for AIS updated
- Land water storage now ends Dec 2016; i.e. +1yr compared to v1 analysis; new parameters included in the model, e.g. glacier mass change

Relevant documents:

<u>SLBC_cci Product Description Document D2.4.2:</u>

Horwath, M.; Novotny, K.; Cazenave, A.; Palanisamy, H.; Marzeion, B.; Paul, F.; Döll, P.; Cáceres, D.; Hogg, A.; Shepherd, A.; Otosaka, I.; Forsberg, R.; Barletta, V.R.; Simonsen, S.; Andersen, O.B.; Rose, S.K.;Ranndal, H.; Johannessen, J.A.; Raj, R.P.; Gutknecht, B.D.; Merchant, Ch.J.; von Schuckmann, K.: *ESA Climate Change Initiative (CCI) Sea Level Budget Closure (SLBC_cci). Product Description Document D2.4.2: Version 2 data sets and uncertainty assessments*. Version 1.2, 18 Jun. 2019.

1.2 Document Structure

Chapter 2 discusses the global ocean mass budget as part of the global mean sea level (GMSL) change. Within this chapter, sources of ocean mass change (glaciers, ice sheets and hydrology) are compared to observed ocean mass changes. The subsequent Chapter 3 puts the GMSL into focus by looking at the mass and the steric component in GMSL change. Chapter 4 discusses the budget of the Arctic Ocean as a regional study within the SLBC_cci project.

1.3 Scientific Background

Sea level change, one of the best indicators of climate change, integrates the response of several components of the Earth system (ocean, atmosphere, cryosphere and hydrosphere) to anthropogenic and natural forcing. Studying the sea level budget helps to better understand processes at work and follow temporal changes (e.g., acceleration) of individual components. It increases our understanding on uncertainties of different observing systems and models. It also allows placing bounds on poorly known contributions (e.g., deep >2000 m ocean warming, not measured by current observing systems), constraining current Earth's energy imbalance and validating climate models used for simulating future climate. GMSL change as a function of time t is usually expressed by the sea level budget equation:

$$\Delta SL(t) = \Delta M_{Ocean}(t) + \Delta SSL(t) \qquad \text{[Eq. 1]}$$

where $\Delta SL(t)$ refers to the change in sea level, $\Delta M_{Ocean}(t)$ refers to the change in mass of the oceans and $\Delta SSL(t)$ refers to the steric contributions, namely the sum of ocean thermal expansion and the halosteric contribution, where in a global mean, the latter is zero due to global salinity conservation.

A major proportion of sea level change is due to the fact that water masses from land get re-distributed into the global ocean. The main sources are known to be melting glaciers and polar ice sheets, but also the variability in the onshore water masses budget has significant impact on sea level changes.

The ocean mass budget reads

$$\Delta M_{Ocean}(t) = -[\Delta M_{Glaciers}(t) + \Delta M_{GIS}(t) + \Delta M_{AIS}(t) + \Delta M_{LWS}(t) + \text{other}], \qquad \text{[Eq. 2]}$$

where $\Delta M_{Glaciers}(t)$, $\Delta M_{GIS}(t)$, $\Delta M_{AIS}(t)$ and $\Delta M_{LWS}(t)$ are the temporal changes in mass of glaciers, Greenland (GIS) / Antarctica (AIS) ice sheets and total land water storage (LWS), including seasonal snow cover. Other terms (e.g., atmospheric water vapour variability) were not considered in this assessment. The mass budget misclosure, as used in this report, is

$$\text{misclosure} = \Delta M_{Ocean}(t) + [\Delta M_{Glaciers}(t) + \Delta M_{GIS}(t) + \Delta M_{AIS}(t) + \Delta M_{LWS}(t)], \qquad \text{[Eq. 3]}$$

where the terms on the right-hand side in Equation 3 now are the assessed mass changes of the respective components, including their errors.

2 Ocean Mass Budget

2.1 Data update

For this chapter of the report, we analysed four different GRACE-based solutions of observed global ocean mass changes, with three different GIA corrections, respectively. In addition to these twelve solutions processed within the project, we also used four external products for comparison. All OMC products and the contributing terms of the named components on the right side of Equation 2 in the previous section are taken from the SLBC_cci version 2 data pool as described in the Product Description Document D2.4.2. For any conversion from OMC or ocean mass contributions to equivalent sea level, 1 Gt corresponds to 1/361 mm equivalent sea level. "Other terms" according to Equation 2 (e.g., atmospheric water vapor variability) were not considered in this assessment.

WP223 Ocean mass change from GRACE (see Figure 2.1). The mass change of the Global Ocean can be determined by its direct effect on the gravity field. Here, we used GRACE Release 06 and ITSG-Grace2018 monthly gravity field solution by means of spherical harmonics up to degree and order 60. Degree-1 coefficients (centre of mass) and $C_{2,0}$ (Earth 'flattening') were replaced with that from satellite laser ranging. We used an un-smoothed ocean integration kernel over the global ocean after applying a 300 km wide coastal leakage buffer. The GAD (AOD1b) background field was restored for each grid cell and month, respectively. The mean atmospheric surface pressure at sea level was subtracted for each month after integrating the GAD over the entire (i.e. unbuffered) global ocean. For details, see Horwath et al. (2019).

Ocean mass time-series from twelve solutions as described in D2.4.2 were used:

- “WP223 Main product” ITSG-Grace2018 spherical-harmonics based solution, with GIA corrections after A et al. (2013), Peltier et al. (2015) and Caron et al. (2018); globally integrated, buffered and scaled time series.
- CSR-, GFZ- and JPL spherical-harmonics based solution, each with A et al. (2013), Peltier et al. (2015) and Caron et al. (2018) GIA correction; identical method to the 'main product'; globally integrated, buffered and scaled time series.
- One mascon solution by the Goddard Space Flight Center (GSFC, Luthcke et al., 2013) dedicated for ocean mass research; globally integrated and scaled geodesic grid product. Used for comparison.
- Chambers’ OMC time-series for CSR, GFZ and JPL; spherical-harmonics based, globally integrated, buffered and scaled time series (Johnson and Chambers 2013, updated). Used for comparison.

We have rescaled the obtained mass changes from a 300 km leakage-buffered ocean onto a common global ocean area of 3.61e+14 m².

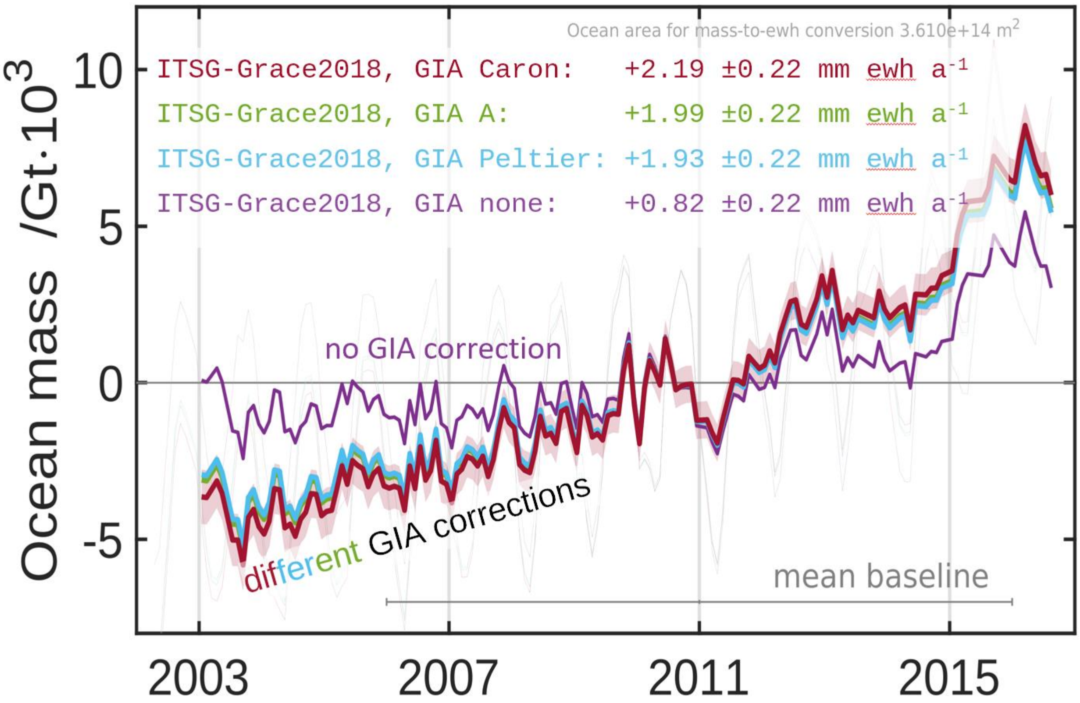

Figure 2.1: GRACE global ocean mass change (OMC) derived from the ITSG-Grace2018 solution with different GIA corrections applied. The light red coloured uncertainty band shows the 1-sigma range for the individual solution with GIA correction after Caron et al. (2018). All curves are plotted with respect to the Jan 2006 to Dec 2015 mean ('baseline'). For the bold curves we removed the annual and semi-annual cycle by subtracting the respective Sine and Cosine content of a multi-parameter adjustment from the original data (shown in faint colours in the background). The uncertainty near the reference date (Jan 2011) is dominated by the solution's individual noise level and increases – due to common trend uncertainty components (i.e. Degree-1, $C_{2,0}$, GIA, leakage) – with distance in time relative to the reference data, which is the mean of the baseline (here: 2011.0). Thus, a systematically larger uncertainty far from the reference date does not reflect data quality but allows for larger divergence between curves there due to trend uncertainties.

Our preferred solution is the ITSG_2018-based solution using the GIA correction according to Caron et al. (2018). We prefer SH-based solutions generated within the SLBC_cci project because this allows full control on the methodology and a full uncertainty assessment. We choose ITSG_2018 as the preferred input SH solution because it shows the lowest noise level among all releases, with no evidence of differences in the contained signal (Groh et al. 2019). We prefer the GIA correction according to Caron et al. (2018) because it is based on the ICE-6G deglaciation history (Peltier et al. 2015), while the model by A et al. (2013) is based on its predecessor model ICE-5G. Furthermore, while the model by A et al. (2013) is a single GIA model, the solution by Caron et al. (2018) arises from a large ensemble of models, where the glaciation history and the solid Earth rheology have been varied and tested against independent geodetic data to provide probabilistic information. This probabilistic information was used to calculate a weighted mean of the individual GIA models, which is what we call the "Caron et al. 2018 solution".

In our analysis for D2.3.2 we found that the (correct) consideration of background models over the entire Global Ocean leads to weaker OMC trends than over the (coastal-) buffered and re-scaled ocean only. See Data Description Document D2.3.2 and Uebbing et al. (2018) for details.

WP233 Glacier mass change (see Figure 2.2): Integrated mass change time series with monthly resolution based on SLBC_cci v2 gridded data as documented in the Product Description Document D2.4.2.

The 2003–2016 and 1993–2016 mass change of global glaciers is based on the Open Global Glacier Model with monthly resolution. In our analysis, we count global glaciers without peripheral glaciers of Greenland and Antarctica. Greenland peripheral glaciers from the model were included in a combined Greenland approach together with altimetry. The model uses global glacier outlines from the Randolph Glacier Inventory (RGI 6.0) and is constrained with seven different global reanalysis products and observational data sets regarding the atmospheric boundary conditions.

Measured mass balances of glaciers were used in line with WGMS data in order to calibrate and validate for the global glacier mass change.

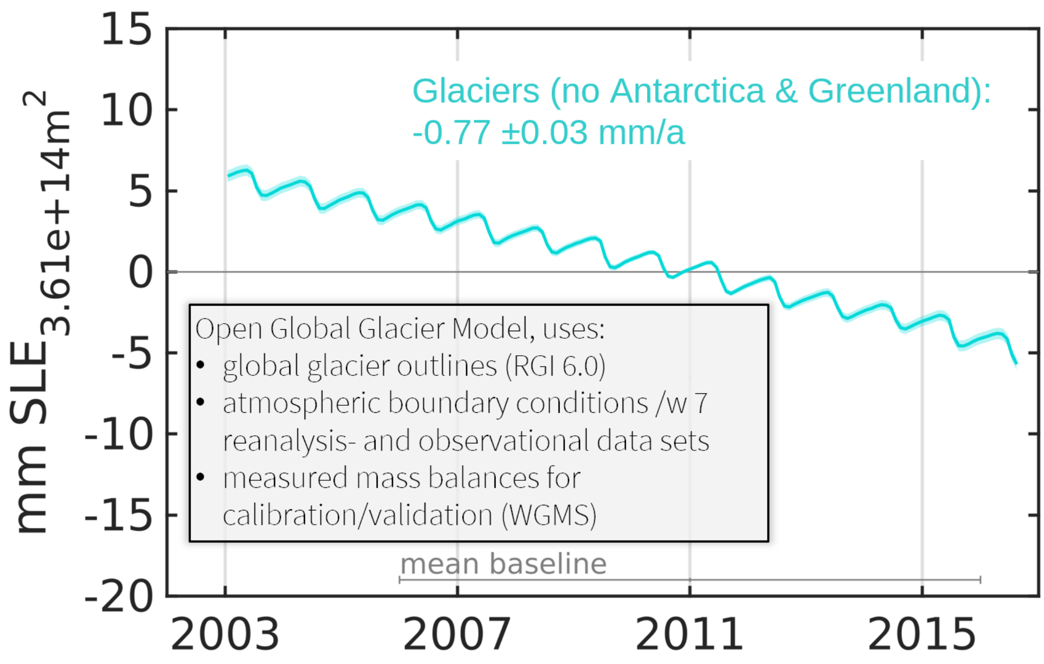

Figure 2.2: Global glacier mass change and uncertainties with respect to the Jan 2006 to Dec 2015 mean. A negative trend means net mass loss of glaciers, i.e. mass gain for the global ocean. Antarctica and Greenland are excluded.

Uncertainties were originally given as half width of the 90 percent confidence interval. To convert them to standard uncertainties (standard deviation of the error), here the numbers were divided by 1.645, based on the assumption of a normal distribution of the errors. Trend uncertainteis were determined from the uncertainties of the annual mass balances of the years involved in the trend calculation. The root sum square (RSS) of the annual mass balance uncertainties, divided by the number of years, was taken as the trend uncertainty, following the suggestion in the D2.4.2 Product Description Document (Horwath et al. 2019, Section 5.4.3) that "the model errors are spatially and temporally uncorrelated".

WP243 Ice sheets mass change:

- GIS (see Figure 2.3). In order to assess mass changes over entire Greenland, we followed two independent approaches:
    - We applied monthly GRACE solutions from the ESA Greenland Ice Sheet CCI project based on CSR GRACE RL06 (GRACE Gravimetric Mass Balance, GMB), which includes mass changes of entire Greenland. This also includes peripheral glaciers and ice caps not directly joint with the Greenland Ice Sheet. We used the GMB integrated mass change time-series for entire Greenland (GIS00_grace.dat) as documented in the Product Description Document D2.4.2. Uncertainties of the trends were taken from the file and from Table 6.1 of D2.4.2. The expected range of accuracy errors of 9 Gt/yr given there translates into 0.025 mm/yr sea level An individual monthly GRACE error (cf. 'noise' for the other GRACE data in this chapter) was included.
    - In a second approach we combine a radar-altimetric record over the Greenland Ice Sheet with mass change information of the peripheral glaciers (connectivity levels 0 and 1) from the Opem Global Glacier Model (WP233). The radar-altimetric record is calibrated to ICESat laser altimetry 2003–2009, but is restricted to the ice sheet only. Combining it with the OGGM results for peripheral glaciers, the result is consistent with the GRACE GMB approach in assessing all ice mass changes on Greenland. The dataset is given as monthly rates. It is plotted in terms of cumulative change in Figure 2.3 (light blue curve).

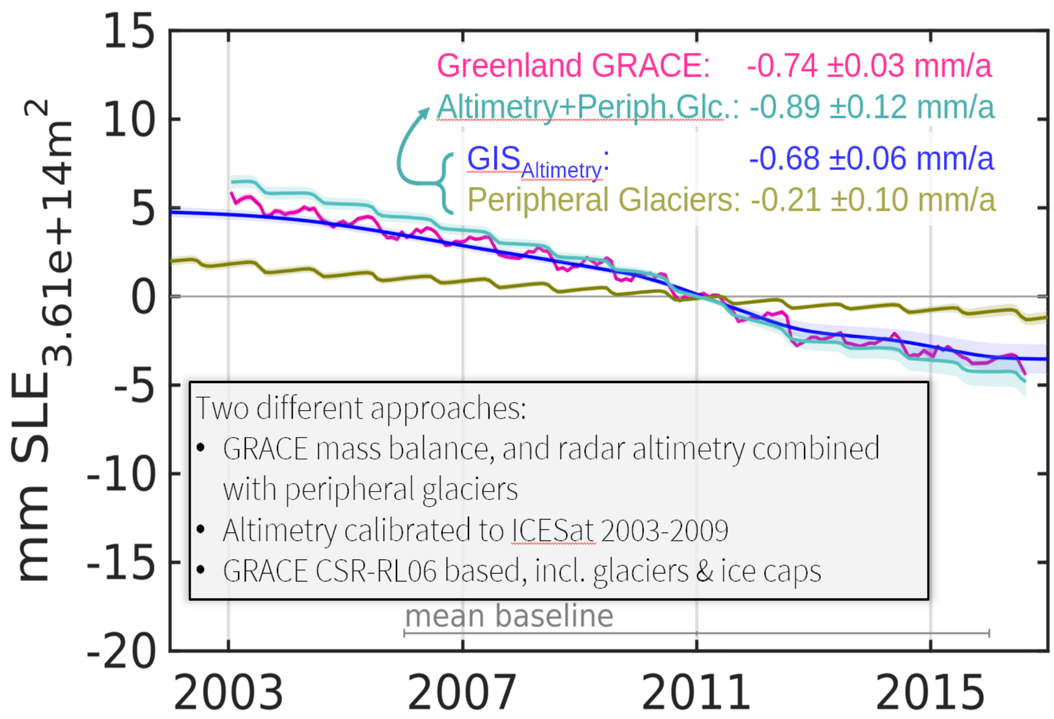

Figure 2.3: Greenland Ice Sheet (GIS) mass change from different sources: GRACE gravimetric mass balance (purple), lidar-calibrated radar altimetry (blue) and peripheral glaciers from global glacier model (brown). Altimetry- and glacier-data were combined (green) to be spatially consistent with GRACE data.

- AIS (see Figure 2.4). Similar to the Greenland Ice Sheet, we followed two approaches in order to determine mass changes of Antarctica over the 2003–2016 period:
  - GMB integrated mass change time series for entire Antarctica (AIS_GMB_basin.dat, AIS32; from the Antarctic Ice Sheet CCI) based on a regional integration approach with tailored kernels, as documented in the Product Description Document D2.4.2. Uncertainties of the trends were taken from Table 6.2 of D2.4.2 and from an additional data file provided with v2 (AIS_GMB_trend.dat).
  - Radar-altimetry record with time-evolving ice-density mask that comprises the entire Antarctic continent, including the Antarctic Peninsula. Note that discrepancies between altimetry-based and GRACE-based mass change estimates exist for the East Antarctic Ice Sheet (not displayed in Figure 2.4). They have been observed previously and are not well understood (see, e.g., Shepherd et al. 2018; Schröder et al. 2019). Possible causes are: errors in the GRACE GIA correction, time-variable penetration effects on radar altimetry; imperfect altimetry inter-mission calibration, imperfect altimetry volume-to-mass conversion.

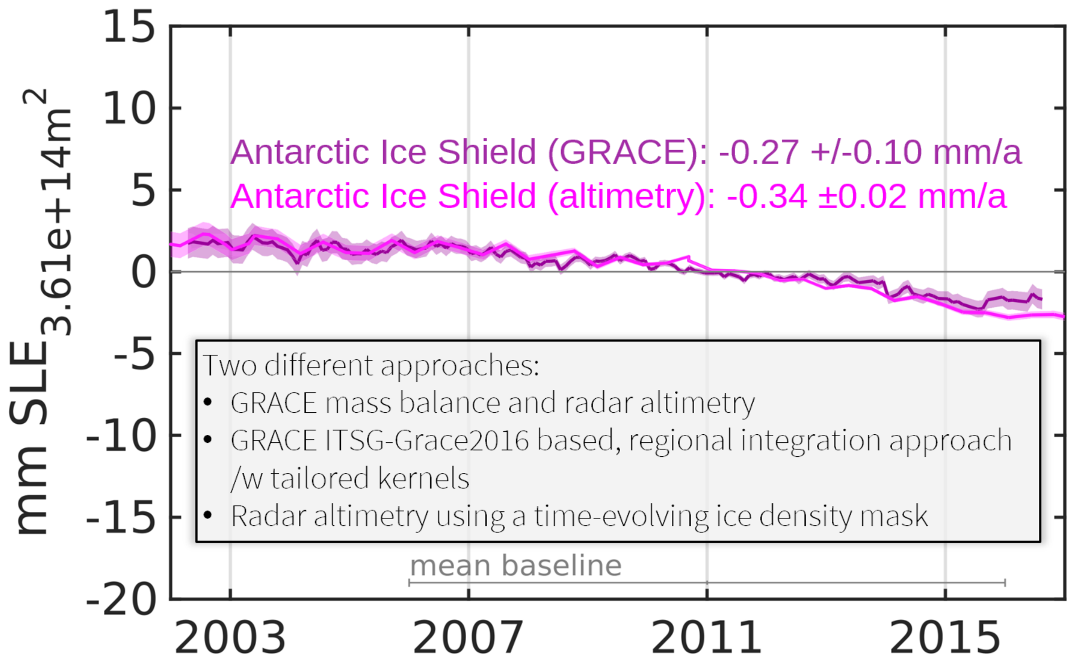

Figure 2.4: Antarctic Ice Sheet mass change relative to the Jan 2006 to Dec 2015 mean with 1-sigma uncertainty bands. Negative trends correspond to mass gain in the Global Ocean

WP252 Land Water Storage Anomaly Net water mass changes on land (see Figure 2.5) were considered using the Global Hydrological Model WaterGAP2.2d (WGHM). Our analysis applies an ensemble mean of different model runs with two irrigation scenarios (70% deficit irrigation and optimal irrigation), and two state-of-the-art climate forcings (WFDEI with GPCC and CRU TS 3.23 precipitation bias-correction). Given monthly time stamps were treated as mid-of-month (representing the mass change of each month, respectively). For the land water contribution, no uncertainty assessment is directly available. We have chosen to estimate the uncertainty of the multi-year trend according to the standard deviation of the ensemble-member trends. Analyses in this chapter, unless otherwise specified, use the ensemble mean of the four 'standard' time-series of globally averaged total water storage anomalies given as equivalent water heights in D2.4.2 (tws_WaterGap22d[…].txt), rescaled from source area to ocean area.

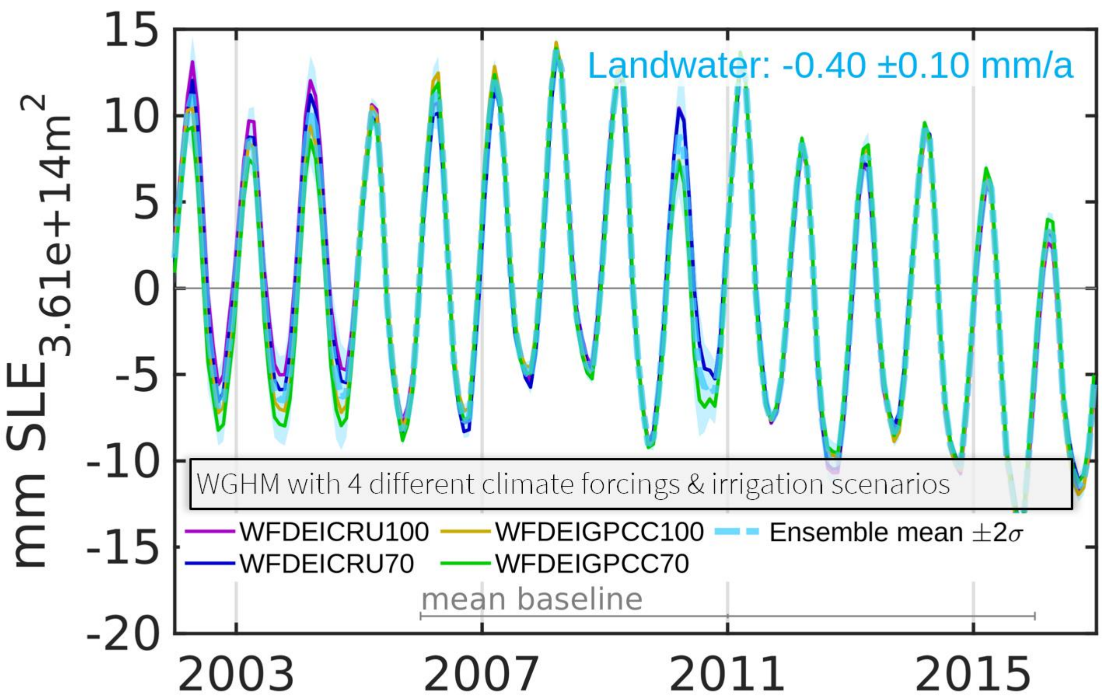

Figure 2.5: Land water storage change with respect to the Jan 2006 to Dec 2015 mean, with negative trends meaning net mass loss off the continents. Note the large seasonal variation in amplitude. The ensemble mean (dashed light blue) is used in the mass budget assessment in this chapter. Also note that multi-annual or decadal oscillations appear to be reflected in the data and may affect trend estimation.

2.2 Budget assessment

2.2.1 Methods

Time series analysis. The time series of contributing components were considered over a common time interval from 01/2003 to 08/2016. While GRACE data have few single 'missing months' starting from January 2011, the time-series are significantly noisier starting in late 2016 from when only Level-2 data including accelerometer transplants from GRACE-A to the GRACE-B satellite are available. At the time of OMC data processing for this project, GRACE Release 06 data and the corresponding correction products (low degree replacements with that from satellite laser ranging and background GAx models) were only provided for until August 2016. Therefore, we do not provide analyses of the Global Ocean mass budget beyond August 2016 in this assessment.

Version 2 data that were given as gridded mass changes over land were globally integrated and scaled onto a common standard ocean surface area of 3.61e+14 m^2.

An un-weighted least squares fit of a 6-parameter function (consisting of a constant, a linear component, an annual cosine and sine function and a semi-annual cosine and sine function) was computed for each restricted mass change time-series based on un-interpolated data, respectively. The linear term of this functional fit is treated as the "trend" and is expressed in units of Gt/yr (gigatonnes per year) for the OMC trend and in mm/yr (millimetres per year) for an equivalent sea level change that corresponds to the OMC. This trend is used for assessing the ocean mass budget. A 'de-trended' time series, or one of which the trend has been removed, is the original time series minus the linear term of the fit.

In a similar manner, we subtract the annual and semi-annual components of the fit from the time-series, whenever a seasonal signal is to be removed. Multi-year cycles with smaller wave numbers, e.g. ENSO effects, are thus still included in the remaining signal (residual).

Annual Sine- and Cosine amplitudes derived from the least squares fit to the individual components furthermore serve as input for analyses of seasonal signals. Data with annual temporal resolution were fitted with the same function but without adjusting for annual and semi-annual components.

The Global Ocean mass budget 2003—2016 was derived from the linear components of ocean mass change and the sum of components, namely Glaciers, AIS, GIS and LWS (cf. Equation 2 and 3). We generated two other sets of time series for purposes of displaying and of analysing the non-linear and non-seasonal components:

- In one set of time series we reduced the annual and semi-annual components.
- In another set of time series we additionally reduced the linear component (trend).

In addition, we then interpolated those time series to a common mid-monthly temporal sampling from 01/2003 to 08/2016. Interpolation is necessary for comparative analyses because of the inhomogeneous time basis of the underlying data products. Based on the common temporal sampling, we calculated the misclosure of the non-linear, non-seasonal components and analysed it statistically, also on a monthly basis. However, the *trends* and analysis of *annual signals* considered throughout this assessment are solely based on original, un-interpolated time series. The same holds true for the evaluation of seasonal amplitudes, which is solely based on analyses of data at original times.

Uncertainties of the trends are taken from D2.4.2. They are considered as standard uncertainties (standard deviation of the error, "one sigma"). Note that these uncertainties exceed the formal uncertainties of the functional fit because their assessment includes systematic effects (e.g. GIA uncertainty, in the case of GRACE-based data products). Uncertainties of sums or differences of the trends from individual contributions are taken as the root sum square of the individual uncertainties. For an assessment on the land water mass trends, we considered the spread between the linear trends obtained from the four land water mass time series that cover the full period 01/2003—08/2016.

Wherever possible in terms of the provided v2 data, we combine uncertainties in the form

$$\sigma_{total}^2(t) = \sigma_{noise}^2(t) + (\sigma_{trend} \cdot (t-t_0))^2 \qquad \text{[Eq. 4]}$$

for time series of mass change $m(t)-m(t_0)$ with respect to a reference time t_0. This means, the uncertainty range at the reference time is σ_{noise} and increases in time before and after t_0. Uncertainties of sums or differences of individual budget contributions contributions (such as for the misclosure) are taken as the root sum square of the individual uncertainties. We note that this error propagation neglects any error correlations between the budget elements. Such correlations exist. For example due to conservation of solid Earth mass, errors of the GRACE GIA correction over ocean are anti-correlated with errors of the same correction over land. However, exploring this kind of correlation is left to future work.

2.2.2 Results for linear trends

The linear trends for all considered terms of the ocean mass budget are given in Table 2.1. For the time interval 01/2003–08/2016, all considered components show a clear positive trend (with positive meaning mass loss on land):

- The **sum of components** amounts to **2.19 +/- 0.15 mm/yr** when GMB results are considered for both ice sheets, and to **2.40 +/- 0.16 mm/yr** when (combined) radar altimetry results are considered. The given uncertainty is the root sum square of individual component uncertainties and an LWS ensemble mean is applied.

- The **Greenland** Ice Sheet contributes with **0.74 +/- 0.03 mm/yr** from GRACE GMB (comprising entire Greenland) and **0.89 +/- 0.12 mm/yr** assessed from radar altimetry and peripheral glaciers combined.
- The **global glaciers** outside Greenland and Antarctica contribute with **0.77 +/- 0.03 mm/yr** and thus contribute similarly to OMC as Greenland.
- The combined **Antarctic Ice Sheet's** contribution as from GMB is **0.27 +/- 0.10 mm/yr**. The corresponding trend derived from altimetry is **0.34 +/- 0.02 mm/yr**.
- The trend in **land water storage** for the ensemble of the four considered model variants amounts to **0.40 +/- 0.10 mm/yr**.

Table 2.1: Mass budget trends 01/2003–08/2016 and their 1-sigma standard uncertainties.

Target	Method	Linear Trend	
Global Glaciers (no Greenland)	OGGM	0.77 ± 0.03	
Greenland (GIS & Periph.Glc.)	GRACE	0.74 ± 0.03	
	Radar altimetry / OGGM		0.89 ± 0.12
Antarctic Ice Sheet	GRACE	0.27 ± 0.10	
	Radar altimetry		0.34 ± 0.02
Land water	TWS anomalies (WGHM)	0.40 ± 0.10	
Sum of mass contributions		2.19 ± 0.15	2.40 ± 0.16
Ocean mass	GRACE	2.19 ± 0.22	
Misclosure (mass budget)	OMC minus sum mass of contributions	0.00 ± 0.29	-0.21 ± 0.30

The OMC trend budget is defined 'closed' when the measured mean ocean mass gain agrees with the sum of mass-losses of contributing components within a reasonable uncertainty range. The trend in mean Global Ocean mass from January 2003 to August 2016 according to our preferred GRACE-based solution (ITSG-Grace2018, Caron's GIA) amounts to +2.19 ± 0.22 mm/a. When GRACE products over the Greenland and Antarctic Ice Shelfs are considered, the sum of mass contributions gives a trend of 2.19 ± 0.15 mm/a; if the altimetry and peripheral glacier products are considered instead, the trend amounts to 2.40 ± 0.16 mm/a (all uncertainties given as 1-σ standard uncertainties).

The corresponding misclosures with combined uncertainties are 0.00 ± 0.29 mm/a (GRACE) and -0.21 ± 0.30 mm/a (altimetry), respectively. It means the mass budget in terms of linear trends is closed within the assessed uncertainty ranges. However, we want to point out that other GIA models (Ice5/6G) may give smaller OMC trends by 0.20 mm/a.

Any closure that is much better than the combined uncertainties may just be a coincidence of trend errors compensating each other.

The observed spread of trends owing to different geodetic and geophysical corrections during the processing of our SLBC_cci v1 and v2 OMC time-series has demonstrated how easily a 'lucky' combination of wrong/insufficient corrections terms and methods may lead to trend values that match the observed sum of components. Table 2.2 illustrates this fact by indicating that the choice of the GIA correction or of the GRACE analysis methodology may alter the results independently by more than 0.2 mm/yr.

Table 2.2: OMC trends [mm/yr w.e.] from different GRACE solutions and different GIA corrections. The first four lines of data show results from different SH solution series generated within SLBC_cci. The last two lines show external products, namely the ensemble mean from Chambers' OMC time series and the GSFC mascon solution. Each column uses different GIA corrections as indicated in the header line. The preferred solution is printed in bold font.

	GIA from A et al. (2013)	GIA from Peltier et al. (2015)	**GIA from Caron et al. (2018)**
ITSG-Grace2018	1.99 ±0.22	1.93 ±0.22	**2.19 ±0.22**
CSR RL06 sh60	1.97 ±0.22	1.91 ±0.22	2.17 ±0.22
GFZ RL06 sh60	1.90 ±0.22	1.84 ±0.22	2.10 ±0.22
JPL RL06 sh60	1.99 ±0.22	1.93 ±0.22	2.19 ±0.22
Chambers ensemble	2.17 ± n/a	n/a	n/a
GSFC v2.4 mascons	2.25 ± n/a	n/a	n/a

2.2.3 Analysis of the Seasonal Mass-Change Budget

Given the sub-annual temporal data resolution of contributing components and GRACE data, we also investigated the seasonal mass change signal; i.e. the degree of agreement between the annual sine and cosine amplitudes of the assessed mass contributions and the GRACE OMC time series (Figure 2.6). Although both time series are almost in phase, we find a small systematic lag: GRACE OMC appears to be approximately 7 days delayed w.r.t. the sum-of-components. Sources of the offset have not been studied conclusively. They might include biases from GAD processing, coastal buffers, leakage effects, water storage modelling or even effects from atmospheric water vapor.

Replacing the land-water ensemble with individual land-water solutions has only marginal effect (on the order of 1 day) on the phase offset. The choice of irrigation scenario is a rather linear effect and has no impact on the phase. Likewise, the choice of the individual RL06 GRACE SH solutions input to our SH-based analysis has no significant effect on the phase. There are, however, significant phase differences with the results of the external GRACE products (GSFC mascons and the Chambers ensemble).

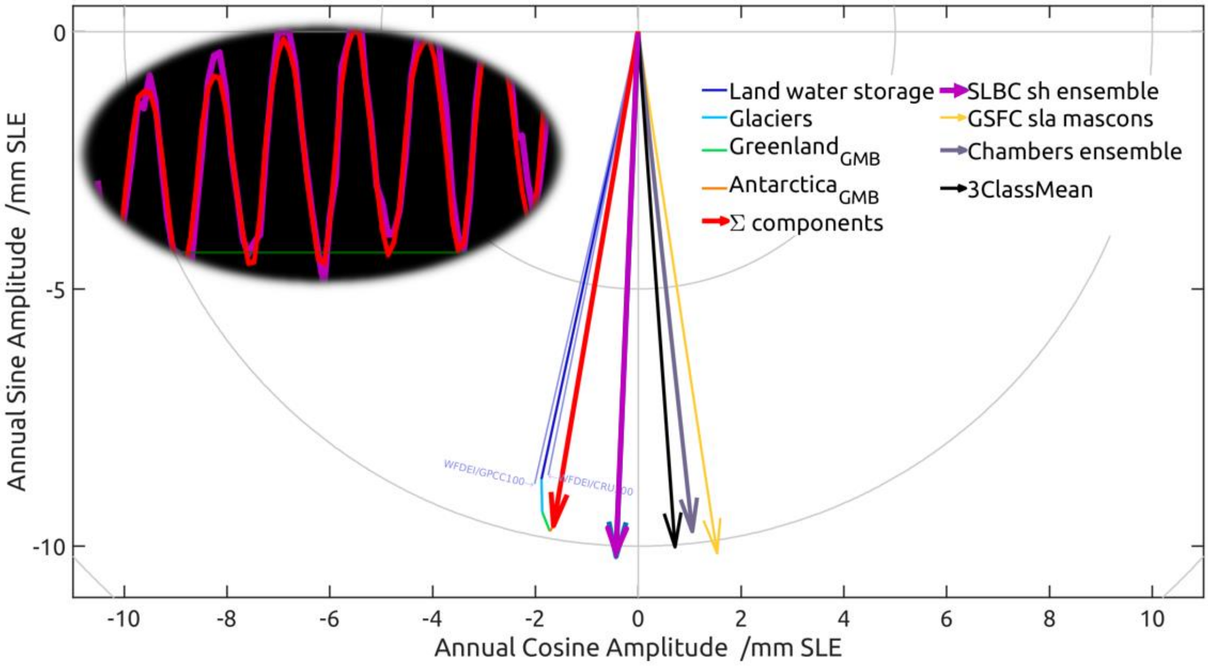

Figure 2.6: Phase diagram of annual sine and cosine amplitudes of various GRACE OMC solutions and of the contributing components. The bold red vector shows the sum of contrbiutions, where the individual contributions are shown as coloured blue and green lines. (Dark blue stands for the TWSA ensemble and the faint blue lines depict the WFDEI/CRU and WFDEI/GPCC forcing variants). The purple vector is the ensemble mean of the SH-based OMC solutions generated by SLBC_cci. The individual SH-based OMC solutions forming this ensemble are not distinguishable below the purple vector. Yellow and grey vectors show external GRACE OMC solutions (GSFC mascons, Chambers' ensemble mean). The black vector shows the mean over the three types of GRACE OMC solutions. The phase difference between the red and the purple vector correponds to 7 days.

2.2.4 Analysis of the ocean mass budget misclosure on the level of individual months

In analogy to the trend misclosure described earlier, we further analysed the monthly mass misclosure, which we define as each month’s Global Ocean mass (GRACE) minus the sum of contributing components in the same month. Figure 2.7 displays the deseasonalized time series of GRACE-based OMC and the sum of mass contributions (GRACE-based for AIS and GIS). The misclosure time series also shown.

The misclosure time series is shown in more detail in Fig. 2.8 together with the 1-sigma, 2-sigma, and 3-sigma uncertainty ranges. We find that 66.5%, 95.1% and 100% of de-seasonalised monthly misclosure are within 1-sigma, 2-sigma, and 3-sigma. This supports the realism of the uncertainty assessment under assumption of a Gaussian error distribution.

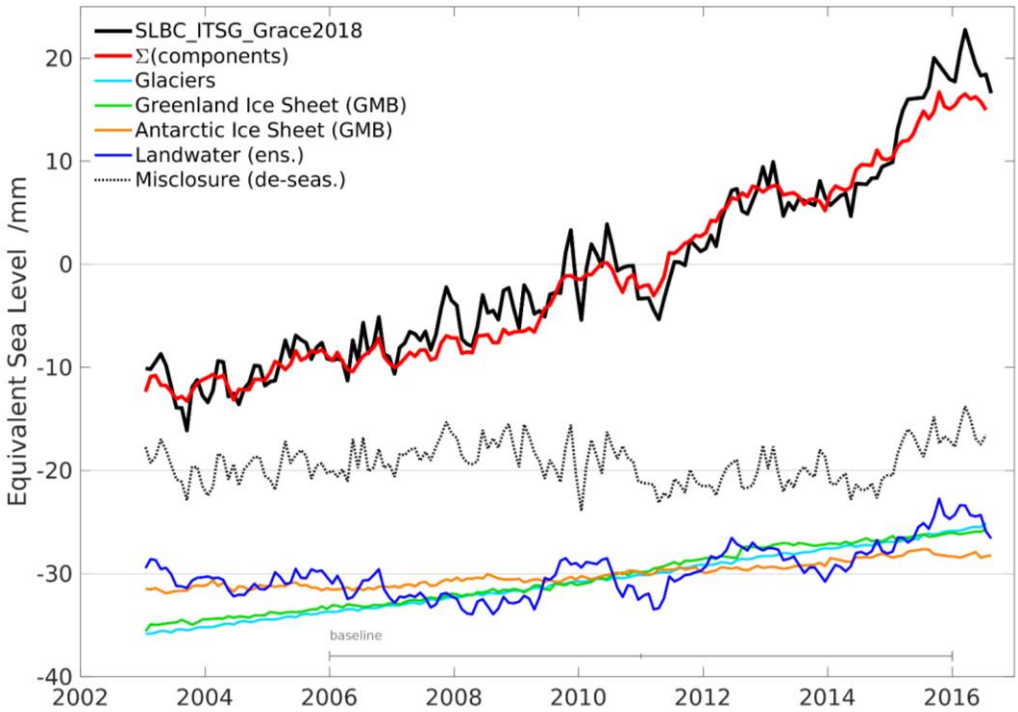

Figure 2.7: De-seasonalised contributing components (bottom, shifted by -20 mm) and GRACE Ocean Mass Change (top). The sum of the contributing components is shown in red. GiaC/A/P: OMC solutions ensemble with GIA corrections after Caron et al. (2018), A et al. (2013) and Peltier et al. (2015), respectively. The black curve is the mean ensemble of all five classes. Note that in this figure the ice sheets mass change was derived from GMB products.

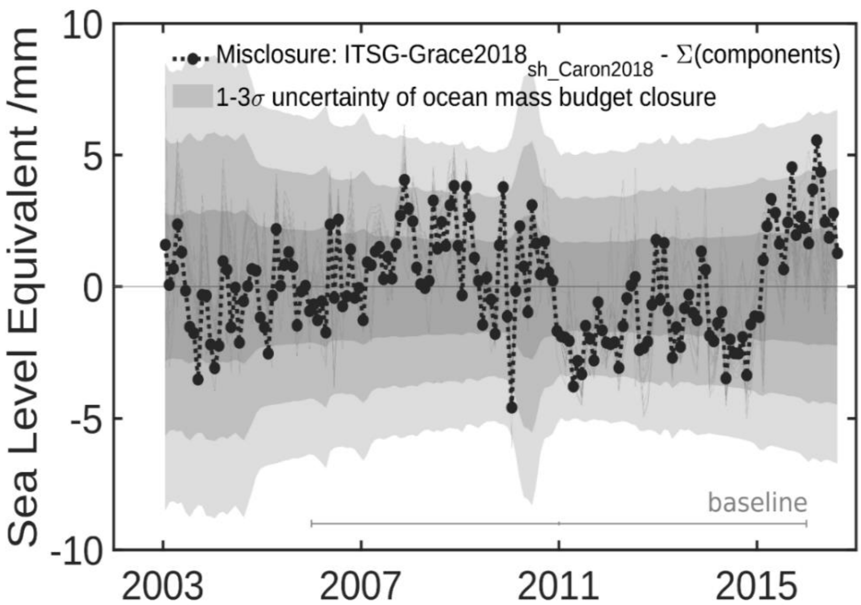

Figure 2.8: Monthly ocean mass misclosure (same as dotted curve in Figure 2.7) plotted on top of the 1—3 σ combined uncertainty. The variety of OMC solutions with different GRACE products and GIA corrections are plotted in the background as faint grey curves.

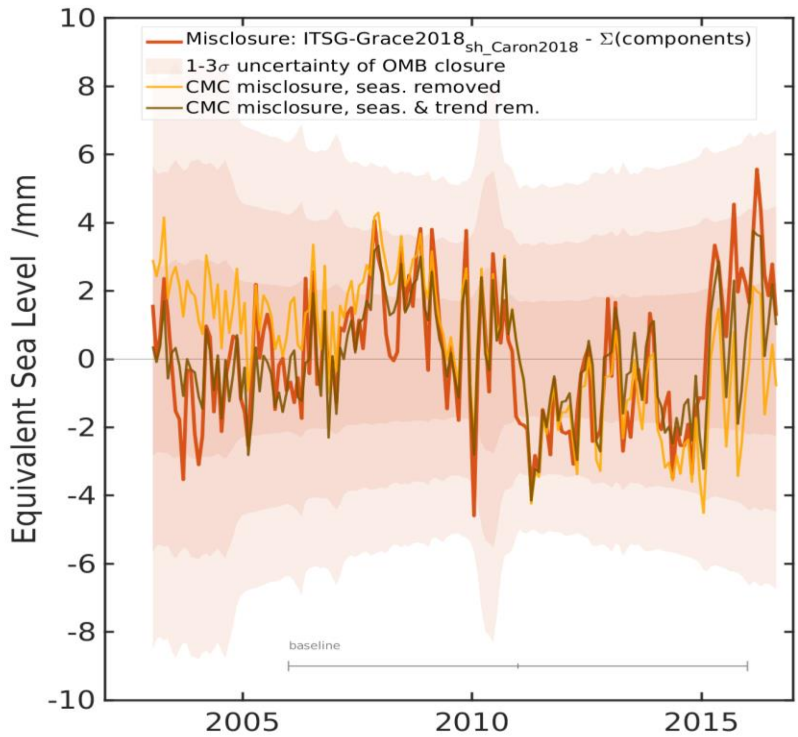

Figure 2.9: Red curve and shaded areas: same as in Figure 2.8. Yellow curve: Difference between GRACE-based continental mass change and the sum of LWS and glacier mass change, with seasonal signal, or seasonal signal and trend, removed, respectively

However, it is obvious from Figure 2.8 that the misclosure has a temporally correlated, interannual characteristics. The only contribution that exhibits interannual variations of sufficient amplitude is the land water storage. We have calculated a continental mass change (CMC) misclosure by taking the difference between the GRACE based CMC product (see D2.4.2 Product Description Document, Horwath et al. 2019) and the sum of the LWS and Glacier products. Figure 2.9 compares the ocean mass budget misclosure and the CMC misclosure. The close match between the two misclosure time series on interannual scales supports the hypothesis that differences between WGHM results and GRACE results are responsible for the interannual part of the ocean mass budget misclosure.

2.3 Discussion and Conclusions

The efforts of the SLBC_cci project to analyse data in a common framework have lead to more rigorous results and new kins of results on the ocean mass budget.

For the linear trend over the 2003-2016 period, the ocean mass budget is closed within the 1σ uncertainties. When using our preferred OMC product (ITSG_2018 with GIA correction according to Caron) and GRACE-based or altimetry-based assessments of ice sheet contributions, the misclosure is 0.00 ± 0.29 mm/yr or -0.21 ± 0.30 mm/yr, respectively. We stress that any closure that is much better than the combined uncertainties may just be a coincidence of trend errors compensating each other.

The closure of the seasonal signal has improved from the v1 assessment to the v2 assessment. The SH-based OMC products are ~7 days late, or the sum of components is ~7 days early. Larger phase differences arise with the external GRACE-based OMC products.

Even on the level of the monthly misclosure time series, the misclosure statistics is in agreement with the assessed uncertainties, where the assessed 1-sigma uncertainty is on the order of 2 mm.

The misclosure contains residual interannual signal. Analysis of the continental mass budget indicates that this is due to differences between the land water storage variations as simulated by WGHM and as derived by our SH-based GRACE analysis.

3 Global Sea Level Budget

The sea level budget closure assessment was performed using two approaches: (1) comparison of observed sea level with sum of individual components from SLBC_cci v2, and (2) with SLBC_cci v2 GRACE-based ocean mass for the mass components. Two-time periods were considered:

Period 1 (P(1)): the entire altimetry era, 1993-2016, where the sea level budget closure was investigated by comparing observed rate of sea level rise with the sum of contributions estimated independently.

Period 2 (P(2)): over the Argo/GRACE era, 2003-2016, where the sea level budget closure was investigated by comparing observed rate of sea level first with the sum of contributions as in P(1) and then with the sum of steric and GRACE based ocean mass.

3.1 Data update

The global mean sea level budget assessment over both periods of study has been performed using glaciers, Antarctica Ice Sheet, Greenland Ice Sheet, land water components from the final version (SLBC_cci v2) of the SLBC_cci project. Detailed description on the processing of the v2 products are provided in the D2.4.2 Product Description Document (Horwath et al. 2019).

The annual and semi-annual cycles were removed in all sea level components time series through a least-squares fit of 12-month and 6-month period sinusoids. No interpolation was performed to fill any existing data gaps in the time series. Linear trends were then estimated using the least squares fit methodology on the un-interpolated data without annual and semi-annual cycles.

For the products whose mass components and associated errors are provided in gigatons (Gt) per year, we converted them into mm of sea level equivalent (SLE) by dividing by a factor of 361 (assuming that 361 Gt of ice mass would raise globally the mean sea level by 1 mm approximately). All results below are expressed in mm SLE.

3.1.1 Observed altimetry sea level data

The final v2 altimetry based GMSL data file consists of GMSL time series from the ESA CCI project over 1993-2016 that has been corrected for TOPEX A instrumental drift over 1993 – February 1999 based on Ablain et al. (2017). The gridded CCI data set available at monthly time scale and at 1°x1° resolution over 82°N and 82°S latitudinal range has been averaged over the SLBC_cci standard, i.e. 65°N and 65°S latitudinal range. The Glacial Isostatic Adjustment (GIA) correction of -0.3 mm/yr (Peltier, 2004) has been applied to the CCI GMSL time series.

The novelty of the v2 data when compared to the previous versions is the availability of a dedicated monthly time step uncertainty estimation (Figure 3.1). The uncertainty data for GMSL time series provided here for SLBC version 2 are obtained from Ablain et al. (2019). The study by Ablain et al. (2019) provides a very detailed explanation for the methodology adapted for the GMSL uncertainty assessment. Three major types of errors are considered in the uncertainty estimation of altimetric GMSL: (a) biases in GMSL between successive altimetry missions characterized by bias uncertainties at any given time; (b) drifts in GMSL due to onboard instrumental drifts or long-terms drift errors such as GIA, orbit, etc. characterized by a trend uncertainty, and (c) other measurement errors such as those due to the geophysical corrections (wet tropospheric, sea state bias, etc.) which exhibit time-variable correlation and are characterized by their standard deviation. These different terms of the GMSL error are combined to build an error variance-covariance matrix. In terms of trend uncertainty, Ablain et al. (2019) estimates the GMSL trend uncertainty to be ± 0.4 mm/yr (90% confidence level, after correcting the TOPEX A drift) which means that at one sigma, the uncertainty is ± 0.24 mm/yr. Figure 3.1 displays the evolution of CCI based GMSL averaged over 65°N and 65°S latitudes after TOPEX A drift correction over Jan. 1993-Feb. 1999. The uncertainty envelope based on Ablain et al. (2019) is in red.

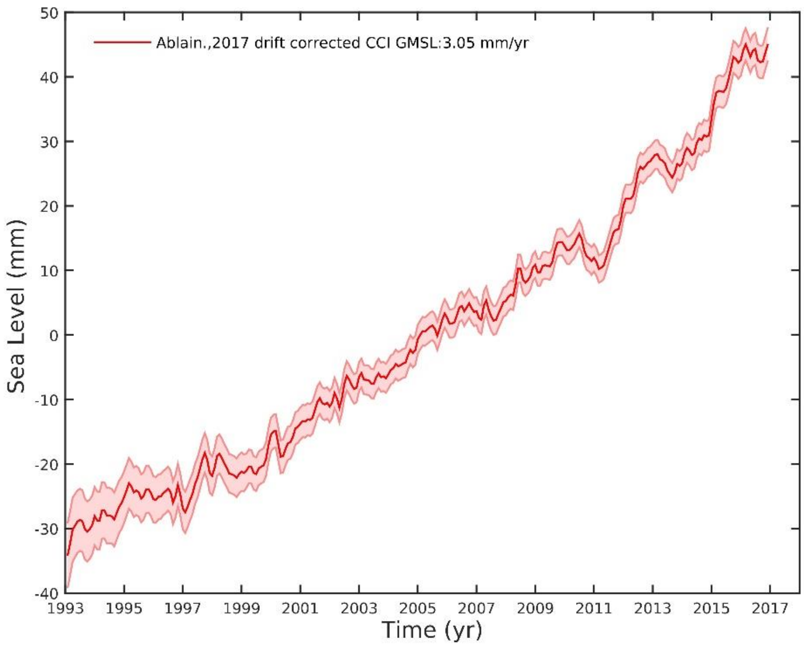

Figure 3.1: CCI based GMSL averaged over 65°N and 65°S latitudes, TOPEX A drift correction over Jan. 1993-Feb. 1999 applied

3.1.2 Individual mass components affecting sea level change

Glaciers

The SLBC_cci v2 glacier mass balance data is based on the glacier evolution model that requires several input variables such as global glacier outlines, atmospheric boundary conditions, measured mass balances etc. (Marzeion et al., 2012). This has then been calibrated and validated using World Glacier Monitoring Service (WGMS, 2016) observational glacier mass balance. The SLBC_cci v2 data base provides two types of monthly data: (1) gridded accumulated glacier mass loss in terms of gigatons (Gt) The global values are obtained by summing over the global grid. (2) Uncertainties of accumulated glacier mass loss also expressed in Gt as global gridded data. Global values of the uncertainty are obtained by taking the square root of the sum of the squares of these uncertainties over the region of interest (globally in this case). In addition to this, the SLBC_cci v2 also provides annual gridded data of glacier mass loss rate, expressed in Gt/yr, as well as the uncertainty of glacier mass loss rate (also in Gt/yr). Glacier trend uncertainty for budget assessment is estimated by taking the mean of the uncertainty of glacier mass loss rate over the periods of interest (i.e. P1 and P2).

Ice Sheets

Greenland Ice Sheet (GIS)

The SLBC_cci v1 database provides two different GIS mass change time series: (1) GIS mass change from radar altimetry and (2) GIS mass change from GRACE. The radar-based GIS time series is the annual mean mass loss for GIS over 1992-2017 and excludes weakly connected ice and peripheral glaciers. The uncertainty is provided in the data product as the standard deviation of the elevation change converted into mass as ice densities. The University of Bremen team has provided the project with estimates of GIS peripheral glaciers mass change time series and this has therefore been considered here and summed with the main GIS data. The GIS trend uncertainty for budget assessment is estimated by taking the mean of the uncertainty of glacier mass loss rate over the periods of interest (i.e. P1 and P2).

The SLBC_cci v2 GRACE based GIS data is identical to the v1 data and is the time series of the mass change data based on the CSR RL06 spherical harmonics-based GRACE release. The uncertainties which are related to the data errors are provided directly with the GRACE monthly models by using a Monte-Carlo-like approach in which 200 simulations were performed. The total trend uncertainty over 2002-2016 accounts to 9 Gt/yr. The GRACE-based v2 solution for the GIS mass change time series is not corrected for GIA. Nevertheless, in our study, we apply the GIA contribution for Greenland mentioned to be -5.4 Gt/yr in the D2.4.2 Document (Page 85) which is based on A et al. (2013)'s ICE5g-VM2 model.

Antarctic Ice Sheet (AIS)

Two AIS mass change time series are available from the SLBC_cci v2 data base: (1) Altimetry-based AIS mass change time series over 1992-2016 available at annual and 140 day epoch time interval and (2) GRACE based monthly AIS mass change time series over 2002-July 2016.

The altimetry based AIS mass change time series comprises data for the East Antarctic, West Antarctic and Antarctic Peninsula ice mass changes derived from radar altimetry and a time evolving ice density mask. The time series available at 140 days epoch is used here and has been linearly interpolated at monthly time scale to correspond to other sea level component time scale. The available time series contain information about time, integrated cumulative mass balance and measurement uncertainty. In addition to this, non-cumulative mass balance uncertainty (in Gt) is also provided in the v2 data set. The trend uncertainty was computed as the gradient of cumulative uncertainty over the period of interest (cumulative year divided by number of years of interest).

The GRACE based Antarctic ice mass change are derived from the spherical harmonic monthly solutions computed by ITSG-Grace2016 by TU Graz (Klinger et al., 2016; Mayer-Gürr et al., 2016) following a regional integration approach with tailored integration kernels that account for both the GRACE error structure and the information on different signal variance levels on the ice sheet and on the ocean (Horwath and Groh, 2016). The GRACE derived mass change time series at monthly intervals are provided for the basin-averaged Antarctic Ice Sheet along with the uncertainty estimates. The trend uncertainty over the Antarctica Ice sheet from GRACE is 38 Gt/yr and is described in detail in the Antarctic_Ice_Sheet_cci Comprehensive Error Characterization Report (Nagler et al., 2017).

Total Land Water Storage

The SLBC_cci v2 provides global averaged and gridded time series of total land water storage (TWS) based on the WaterGAP 2.2d global hydrological model (WGHM) which includes a series of model enhancements (as discussed in product description document D2.4.2) which differentiate from the previous versions. Two variants of WaterGAP 2.2d corresponding to two irrigation scenarios (70% deficit scenario and 100% or optimal irrigation scenario) are provided, each of which uses two climate forcings: daily WFDEI using GPCC precipitation, WFDEI using CRU TS 3.23 precipitation forcing. The time series are available at monthly resolution over 1993-2016. For the sea level budget assessment, we use the ensemble mean of the above mentioned TWS products. The uncertainty over each time step is estimated as the RMS of the 4 data sets from the ensemble mean. The trend uncertainty is the standard deviation of the trend of the individual data sets over the 2 periods of interest.

Figure 3.2 displays the individual SLBC_cci_v2 mass components time series over 1993-2016.

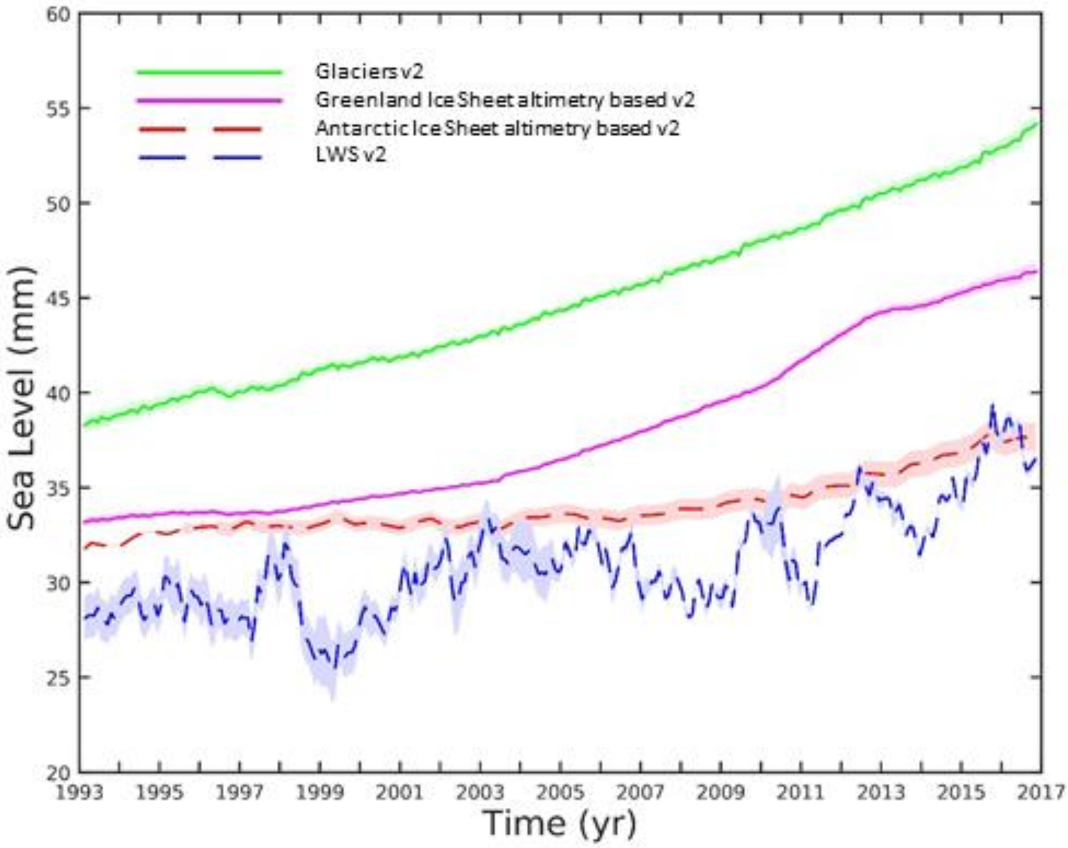

Figure 3.2: SLBC_cci v2 mass components in equivalent sea level (mm) contributing to total sea level over 1993-2016

3.1.3 Ocean mass product from GRACE

The SLBC_cci v2 provides one main product, namely ITSG Grace2018 (Mayer-Gürr et al., 2018a,b) based on a spherical harmonics solution. In addition, several other supplementary v2 products exist, such as spherical harmonics based CSR, JPL, GFZ based on GRACE RL06, GSFC mascon based GRACE (Luthcke et al., 2013) and Chambers based GRACE ocean mass data (Johnson and Chambers, 2013, Chambers and Bonin, 2012). The v2 GRACE products are based on the latest GRACE release (RL06) as compared to v1 GRACE which was based on RL05.

The SLBC_cci v2 main product (ITSG) and other SH based supplementary products provided here have undergone various processing and corrections (refer to D2.4.2, pages 38-44). Furthermore, the spherical harmonics-based solutions have been provided to us with three types of GIA corrections: (1) GIA removal based on A et al. (2013), based on ICE-5Gv2 from Peltier (2004), (2) (2) GIA correction based on Peltier et al.(2015)'s ICE6G_C, VM5a model and (3) GIA removal based on Caron et al. (2018).

Here we consider the globally averaged ocean mass change data from GRACE provided at a monthly resolution between mid-2002 and end of 2016. The globally averaged ocean mass datasets also provide uncertainty values at monthly time steps estimated based on different sources of errors such as GRACE errors, leakage errors, GIA uncertainty etc. Two types of uncertainty are provided: (1) uncertainty due to noise, (2) systematic errors of the linear trend. As mentioned in the D2.4.2 document (page 56-58), the uncertainties at each time step are combined in the form of :

$$\sigma_{total}^2(t) = \sigma_{noise}^2 + \left(\sigma_{trend} \cdot (t - t_0)\right)^2 \qquad \text{[Eq. 5]}$$

for time-series of mass change $\Delta M(t)$-$\Delta M(t_o)$ with respect to a reference time t_o.

Figure 3.3 displays the GRACE based ocean mass time series over 2003-July 2016 from various processing groups with the three different GIA corrections applied. Their corresponding trend estimates over the same period of study are indicated in Table 2.1. The trend estimates of the spherical harmonics-based GRACE ocean mass from ITSG (SLBC_cci main product) and from CSR, JPL, GFZ show very similar values over 2003-July 2016. The A et al.(2013) and Peltier et al. (2015)' ICE-6G GIA corrected GRACE data produce identical trend values (differences exits mainly in the second order of the decimal) whereas differences in the order of 0.2 mm/yr arise between the Caron et al. (2018) based data and the two above mentioned GIA correction. Caron et al. (2018) GIA corrected ocean mass exhibits higher range of trend than the A et al. (2013) and Peltier et al. (2015) GIA corrected GRACE ocean mass time series. Comparison with external data such as the GSFC Mascon based ocean mass and Chambers spherical harmonics-based ocean mass show that the ITSG, CSR, JPL and GFZ ocean mass time series corrected with Caron et al. (2018) produce the closest trend values with these externally processed data.

Table 3.1: Trend estimates of GRACE based ocean mass time series over 2003-July 2016

	Trend (mm/yr)	2003-July 2016		
		GIA correction		
		A. et al.,2013	Caron et al., 2018	ICE6G
SLBC v2 principal product	ITSG SH	1.89±0.253	2.18±0.253	1.87±0.253
Supplementary data	CSR SH	1.87±0.253	2.16±0.253	1.86±0.253
	GFZ SH	1.83±0.253	2.12±0.253	1.81±0.253
	JPL SH	1.9±0.253	2.19±0.253	1.88±0.253
	GSFC Mascon	2.11		
	Chambers et al., CSR SH	2.23		
	Chambers et al., GFZ SH	2.01		
	Chambers et al., JPL SH	2.25		

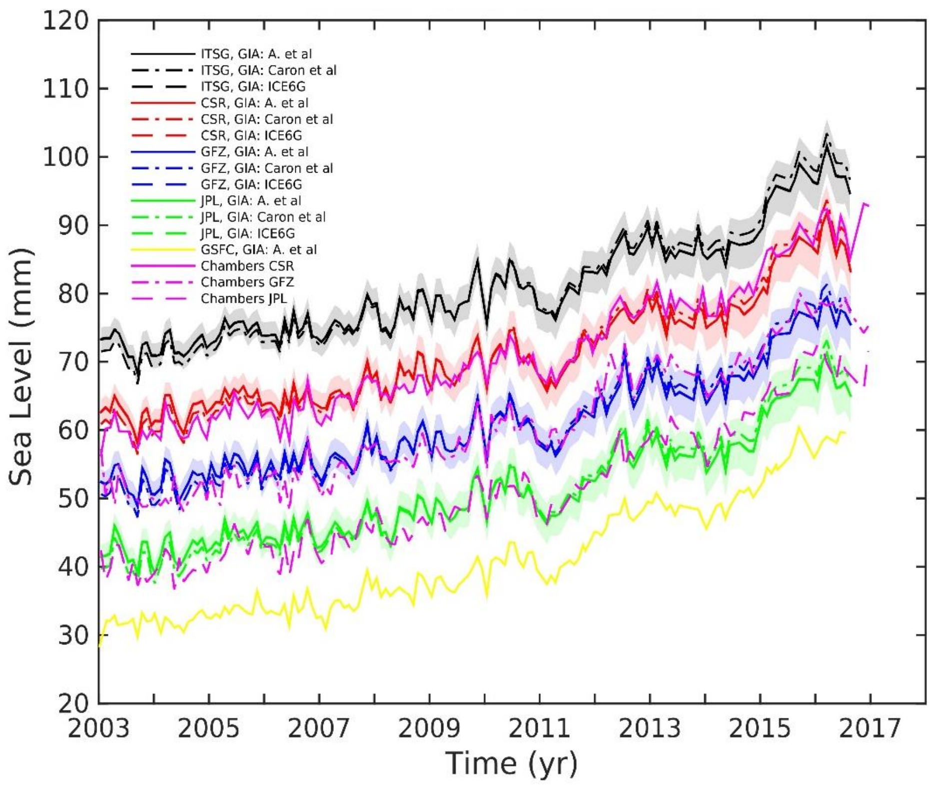

Figure 3.3: GRACE based ocean mass contribution in mm from various processing groups with three different GIA corrections over 2003-2016. The main SLBC_cci v2 product is ITSG (in black) while all others shown correspond to supplementary GRACE products.

3.1.4 Steric sea level component

The SLBC_cci v2 steric product consists of globally averaged and gridded 5°x5° time series over of monthly mean Steric Sea Level Anomaly (SSLA) based on XBT and XCTD and Argo profiles over 2003-2016. The profiles are processed onto common vertical levels up to a depth of 2000m using an updated version of the box averaging method developed by von Schuckmann and Le Traon (2011). The horizonal resolution has also been refined in the recent version. SLBC_cci adopted 2006 to 2015 inclusive as the baseline period for calculation of anomalies. The EN 4.2.1 climatology used here is therefore the average for each month of the year of the EN 4.2.1 analysis for that baseline period. The SLBC_cci v2 steric data covers only until the depth of 2000m. therefore deep ocean steric trend contribution of 0.1 ± 0.1 mm/yr based on Purkey and Johnson (2010) is considered in the budget assessment along with the contribution until 2000m depth.

Uncertainty estimates are provided at each time step and are estimated based on uncertainty in measurement of temperature, salinity sea surface temperature, parametric uncertainty and uncertainty due to under-sampling geophysical variability (Page 36 of D2.4.2). Trend uncertainty is estimated as the root sum square of the gradient of time step uncertainty over the period of interest and the deep ocean contribution uncertainty of 0.1 mm/yr.

Since the steric SLBC_cci v2 product is available only from 2003, it is therefore used for P(2) budget assessment whereas over the P(1) period, steric data from Dieng et al., 2017 at monthly time scale and thermosteric sea level data from WCRP Global Sea level Budget group (2018) at annual time scale have been used (Figure 3.4a). Comparison of SLBC_cci v2 steric data with WCRP Global Sea level Budget group (2018) is in Figure 3.4b.

The thermosteric time series estimated until the depth of 2000 m from WCRP (2018) is an ensemble mean from 11 different processing groups that have used XBTs and CTDs during the pre-Argo era (i.e. from 1993 until 2003/2005), followed by Argo floats data until 2015. Deep ocean contribution of 0.1 mm/yr has also been included in this data set. Detailed explanation on the data sets used and the processing can be found in WCRP Global Sea level Budget group (2018). The ensemble mean steric time series from Dieng et al. (2017) comprises the following three data sets for the period 1993-2004: the updated versions of Ishii and Kimoto (2009), NOAA data set (Levitus et al., 2012) and EN4 data set (Good et al., 2013). Over the recent years, these data sets integrate Argo data from IPRC, JAMSTEC and SCRIPPS. Deep ocean contribution has also been included.

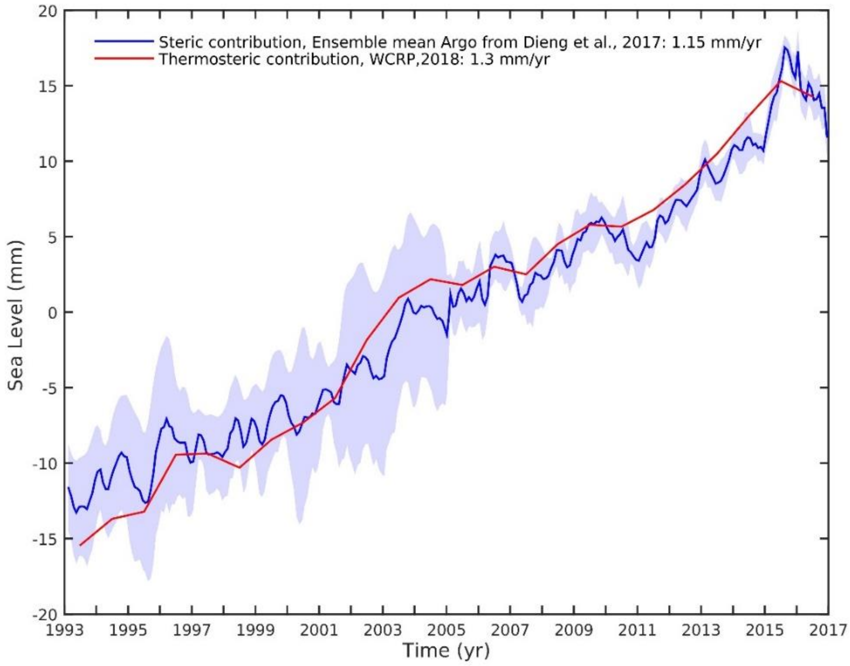

Figure 3.4a: Dieng et al., 2017 steric (in blue) and WCRP, 2018 thermosteric (in red) sea level time series over 1993-2016.

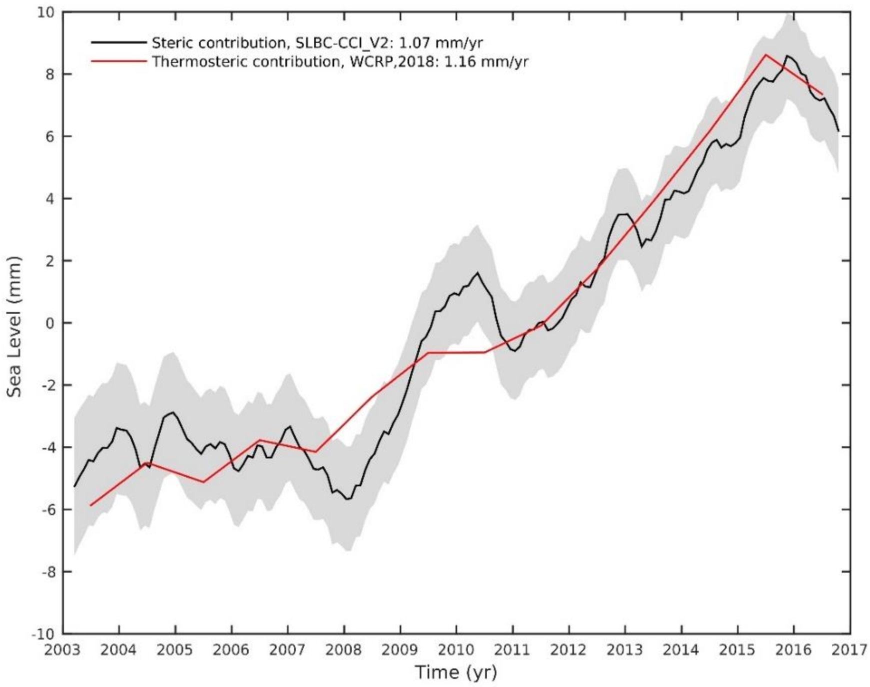

Figure 3.4b: SLBC_cci v2 steric (in black) and WCRP, 2018 thermosteric (in red) time series over 2003-2016.

3.2 Budget assessment

3.2.1 Period P(1): the altimetry era (1993-2016)

The global mean sea level budget was estimated by comparing the GMSL observed by satellite altimetry with the sum of the SLBC_cci v2 components except for the steric sea level component over 1993-2016, where steric data from Dieng et al. (2017) was used. Since the thermosteric data from WCRP, 2018 is at annual time resolution, it is used only for annual sea level budget assessment.

Figure 3.5 displays the global mean sea level change estimated as the sum of individual SLBC_cci v2 components superimposed to the altimetry-based GMSL. Individual components are also displayed. The global mean sea level trend (Table 3.2) obtained as the sum of individual SLBC_cci v2 components over 1993-2016 accounts to 2.91±0.22 mm/yr, whereas observed GMSL trend value accounts to 3.05±0.24 mm/yr leaving a residual of 0.14±0.3 mm/yr. In terms of interannual variability, the GMSL obtained from the sum of components corresponds well with observed altimetry-based CCI GMSL, except in the beginning years. This is expected, as the TOPEX A drift correction between 1993 and 1998 is not yet precise. In addition to this, we can also observe the high uncertainty range in the sum of components time series initially until 2005. This high range of uncertainty is mainly due to the steric component (which also exhibits high uncertainty range between 1993 and 2003) as it is based on XBT data over 1993-2003/2005 and therefore suffers from sparse coverage both geographically and at depth (below 700 m). The RMS of the residual time series over 1993-2016 amounts to 2.2 mm.

Table 3.2: Observed GMSL trend compared with sum of components trend over 1993-2016

	1993-2016	
Budget	Trend (mm/yr)	Uncertainty (mm/yr)
Observed Altimetry GMSL	**3.05**	**0.24**
Steric, Dieng et al.,2017	1.15	0.12
Glaciers	0.64	0.13
Greenland Ice Sheet	0.43	0.038
Greenland Peripheral Glacier	0.17	0.08
Antarctica Ice Sheet	0.2	0.027
Land Water	0.32	0.1
Sum of components	**2.91**	**0.22**
Residual	0.14	0.3
RMS	2.2 mm	

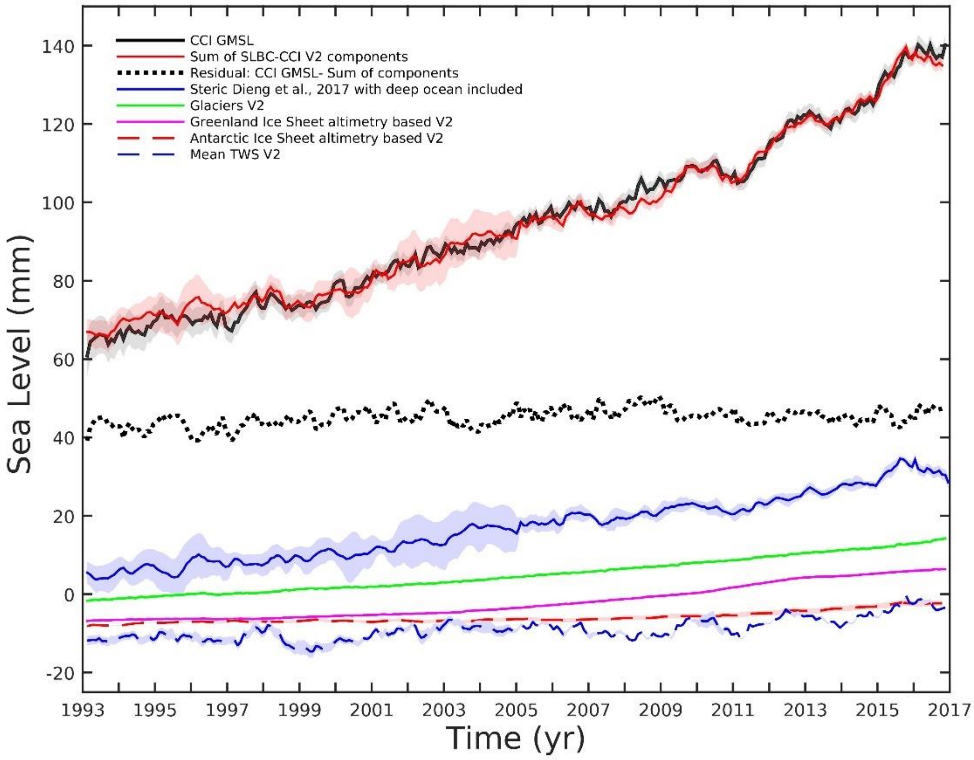

Figure 3.5: Observed CCI GMSL (black) superimposed with the GMSL estimated from the sum of SLBC_cci v2 sea level components (in red) over 1993-2016.The residual time series (i.e. CCI GMSL- sum of components) is shown as dotted black time series. The individual components, steric (in blue), glaciers (in green), Greenland (in magenta, altimetry-based), Antarctica (dashed red, altimetry-based) and TWS (dashed blue) are also displayed.

In addition to the time series and trend based sea level budget assessment, annual sea level budget was also assessed. Figure 3.6 displays the annual sea level budget based on SLBC_cci v2 mass components and WCRP, 2018 thermosteric component and compared with the observed altimetry sea level. We can notice that for most of the years between 1993 and 2016, the annual budget remains closed. Certain years show a small range of residual signal which is within the combined uncertainties. Performing the same assessment using Dieng et al. (2017) steric data instead of the WCRP Global Sea level Budget group (2018) also yields similar results, and hence is not shown.

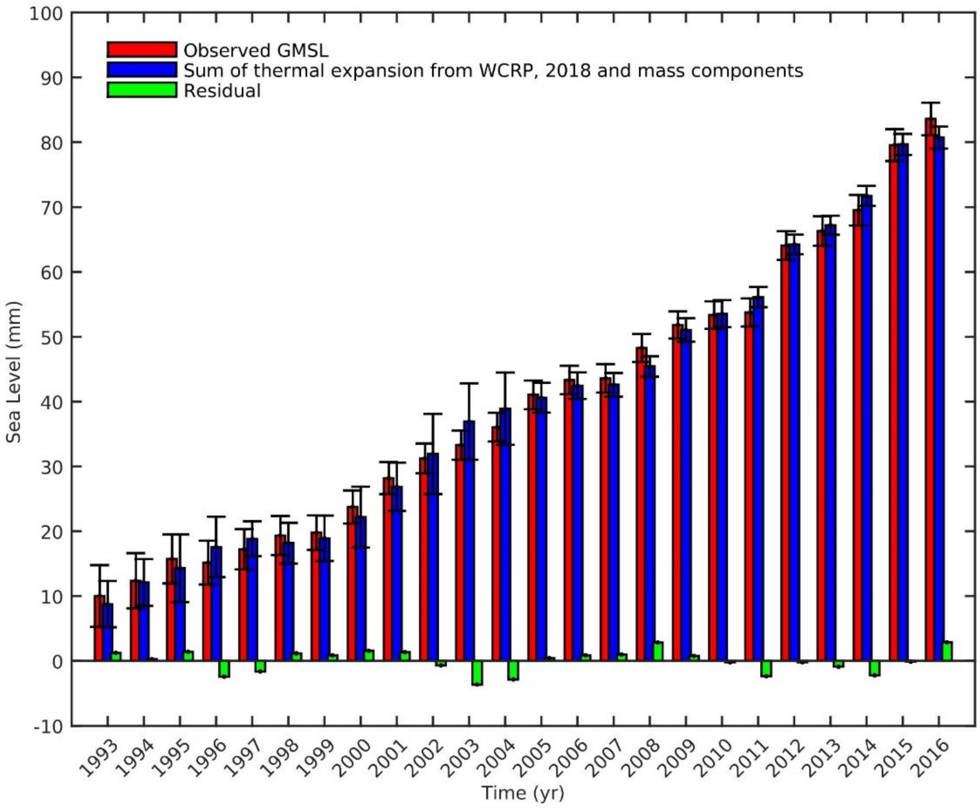

Figure 3.6: Annual sea level budget analysis over 1993-2016 using SLBC_cci v2 sea level components

3.2.2 Period P(2): the Argo/GRACE era (2003-2015)

For this time period, the sea level budget closure was investigated by comparing observed GMSL first with the sum of individual SLBC_cci v2 sea level components as in P(1) (explained in the previous section) and then with the sum of steric and GRACE based ocean mass. Table 3.3 summarizes the trend value of observed CCI GMSL and sum of each SLBC_cci v2 components contributing to sea level variations over 2003-2016. For the 2003-2016 period, the steric data from this project has been used. Sea level budget assessment over this time period was performed using two different sets of AIS and GIS data: (1) altimetry based, over 2003-2016 complete years (2) GRACE based AIS and GIS contribution over 2003-August2016. In Table 3.3, the GRACE based contributions and henceforth the corresponding sea level budget are shown in italic. From the table, we can observe that the sum of components based on altimetry AIS/GIS contributions is 3.49±0.22 mm/yr and whereas the sum based on GRACE AIS/GIS contributions is 3.32±0.2 mm/yr, respectively, thereby leaving a residual of 0.17±0.32mm/yr and 0.32±0.31 mm/yr respectively. The slightly higher trend residual in the case of GRACE AIS/GIS based budget could be attributed to trend estimation over time period when the complete end year is not accounted for. To verify this, sea level budget assessment was performed over August 2003-August 2016, and the residual trend as a result decreased to

0.24±0.3 mm/yr (instead of 0.32±0.31 mm/yr over 2003-July 2016). Figure 3.7 displays the global mean sea level budget estimated as the sum of individual SLBC_cci v2 sea level components (in red) superimposed to the CCI observed altimetry based global mean sea level time series (in black) over 2003-2015 and its corresponding residual (dotted black line). The individual components are also displayed in the same figure. Altimetry based AIS and GIS time series are depicted in Figure 3.7. (GRACE based time series are also similar and henceforth not shown here).

In addition to trend based sea level budget assessment, annual sea level budget was also assessed. Figure 3.8 displays the annual sea level budget based on SLBC_cci v2 sea level components (altimetry based in the case of AIS and GIS) compared with the observed altimetry sea level. We can notice that the annual sea level budget residual is higher in the initial years after which the residuals are lower.

Table 3.3: Observed CCI GMSL trend compared with sum of components trend over 2003-2016. GRACE based AIS and GIS contributions and their corresponding budget trend values are in italic

	2003-2016/*2003-July 2016*	
Budget	Trend (mm/yr)	Uncertainty (mm/yr)
Observed Altimetry GMSL	3.66/*3.64*	0.24
Steric UoR v2	1.07/*1.09*	0.1
Glaciers	0.77	0.13
Radar GIS including peripheral/ *GRACE GIS*	0.88/*0.77*	0.11/*0.02*
Radar AIS/ *GRACE AIS*	0.35/*0.28*	0.02/*0.1*
Land Water	0.42/0.41	0.1
Sum of components	3.49/*3.32*	0.22/*0.2*
Residual	0.17/*0.32*	0.32/*0.31*
RMS	2.78 mm/*3.1 mm*	

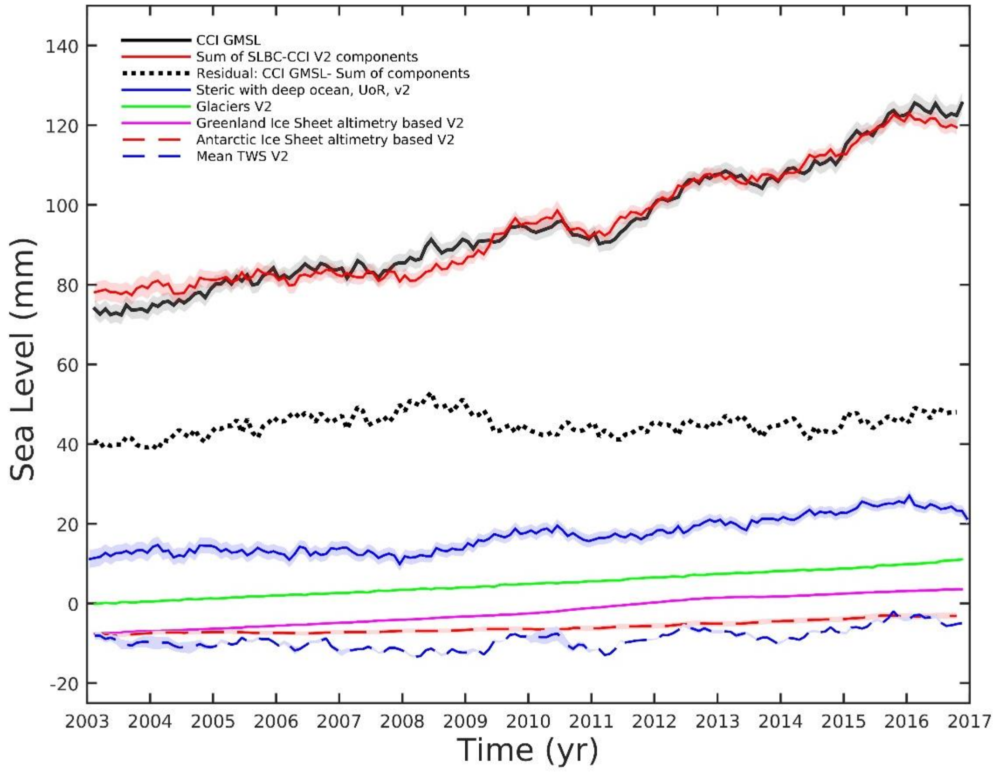

Figure 3.7: Same as in Figure 3.5 but over 2003-2016

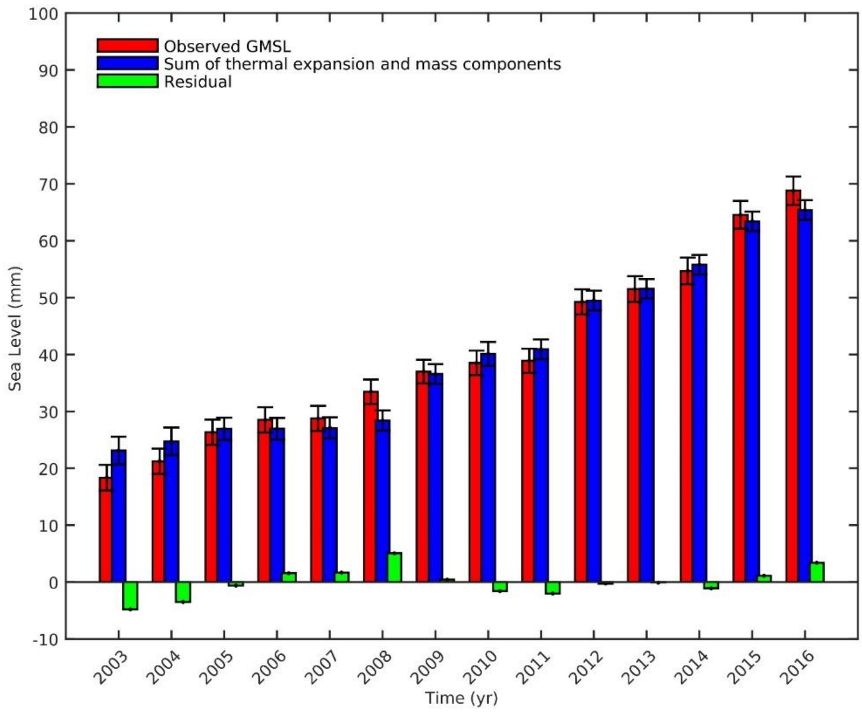

Figure 3.8: Annual sea level budget analysis over 2003-2016 using SLBC_cci v2 sea level components

3.2.3 Sea level budget residual analysis in terms of interannual variability

In Figure 3.7, taking a closer look at the residual curve (dotted black line), we can observe the amplitude of the residual to be slightly higher over 2005-2009. To study this further, we superimposed detrend altimetry based observed GMSL time series with the detrended sum of components time series as shown in Figure 3.9. The residual time series has also been detrended and shown. By detrending the time series, we can obtain time series that contain only its interannual variability. In Figure 3.9, we can observe that there is no correlation between the detrended observed GMSL and detrended sum of components time series between 2003 and 2011 after which both detrended time series are well correlated (>0.8). This non-correlation explains the sea level budget residual being higher during over 2003-2011 than the rest of the period of interest.

In order to identify the sea level component responsible for the sea level budget non correlation in terms of interannual variability over 2003-2011, we adopted the methodology by Dieng et al. (2015). We compared the detrended time series of each sea level component with the inverse (i.e. multiplied by -1) of the detrended residual time series. The two main components that contribute to the interannual variability in global mean sea level are the steric and land water components. The rest of the sea level components: glaciers, AIS and GIS do not contribute to total sea level in terms of interannual variability.

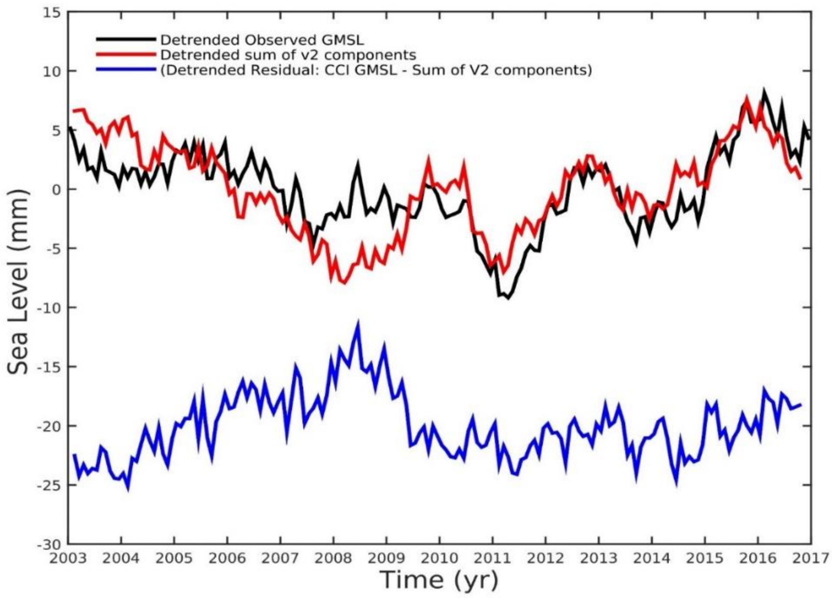

Figure 3.9: Comparison of detrended observed sea level (in black) with detrended sum of components (red). The detrended residual is also displayed (in blue)

Figure 3.10 shows the comparison of the inverse detrended sea level budget residual time series with detrended steric (Figure 3.10a) and detrended land water (Figure 3.10b) components. High correlation (>0.8) between the detrended steric and inverse detrended residual between 2003 and 2010 (visible in Figure 3.10a) shows that it is the steric component that contributes to the sea level budget mis-closure in terms of interannual variability over this period. Similarly, high correlation (>0.8) between detrended land water and inverse detrended residual time series over 2010-2011 (and not before) shows that the land water component contributes to the mis-closure in terms of interannual variability over 2010-2011 (Figure 3.10b).

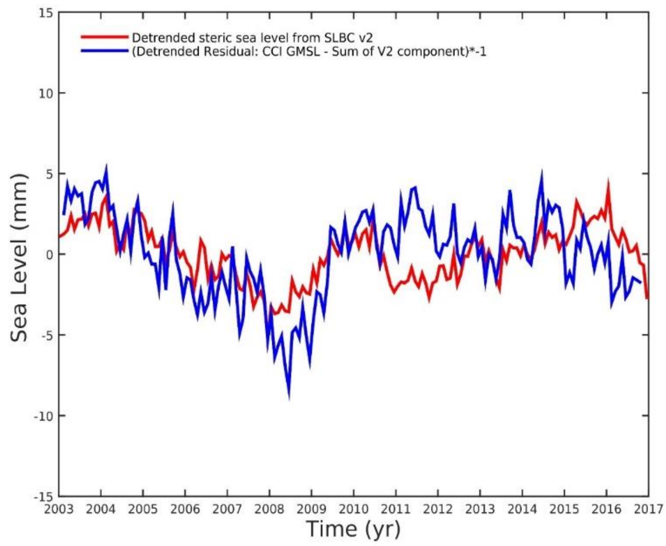

Figure 3.10 (a): Comparison of detrended steric sea level time series with inverse (i.e. multiplied by -1) detrended sea level budget residual.

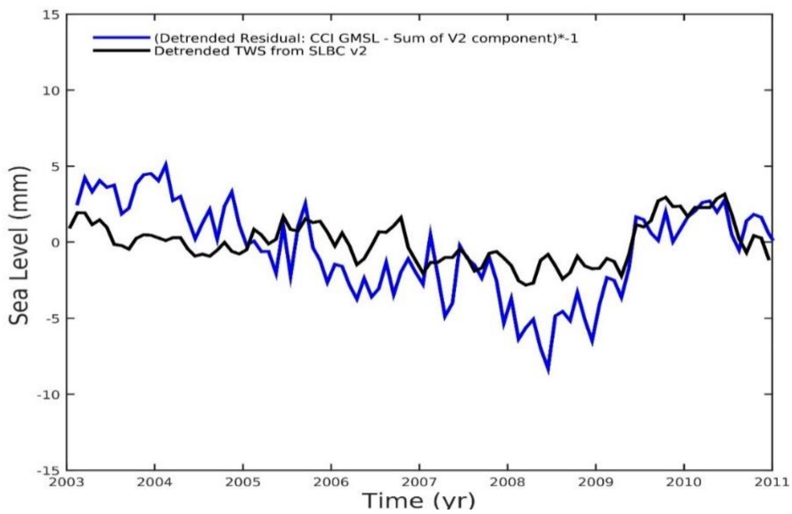

Figure 3.10(b): Comparison of detrended land water time series with inverse (i.e. multiplied by -1) detrended sea level budget residual

3.2.4 Sea level budget using GRACE ocean mass

Over 2003-2016 time period corresponding to the Argo/GRACE era, the individual mass components (glaciers, AIS, GIS, TWS) can be replaced by ocean mass directly observed by GRACE. Therefore, over this time period the sea level budget was also performed using the main and supplementary SLBC_cci v2 GRACE ocean mass products over Jan.2003-Aug.2016. Table 3.4 summarizes their corresponding trend values, residual trends and RMS.

Table 3.4: Observed CCI GMSL trend over Jan. 2003 - Aug. 2016 compared to the sum of components, where the mass component is based on GRACE. Individual columns correspond to different GRACE solutions.

Trend (mm/yr)	**Jan. 2003-August 2016**				
	ITSG A et al.,2013	**ITSG Caron et al., 2018**	**ITSG ICE6G**	**GSFC Mascon**	**Mean Chambers (Global)**
Observed GMSL	3.58±0.24	3.58±0.24	3.58±0.24	3.58±0.24	3.58±0.24
Steric v2	1.07±0.1	1.07±0.1	1.07±0.1	1.07±0.1	1.07±0.1
GRACE	1.89±0.25	2.18±0.25	1.87±0.25	2.11	2.17
Sum	2.96±0.27	3.25±0.27	2.94±0.27	3.18	3.24
Residual	0.62±0.36	0.33±0.36	0.64±0.36	0.4	0.34
RMS (mm)	3.67	2.94	3.7	3.08	2.94

In terms of sea level budget residual trend values, the ITSG GRACE ocean mass based with Caron et al., 2018 GIA correction produces the least residual trend of 0.33±0.36 mm/yr and RMS of 2.94 mm. Figure 3. 11 displays the sea level budget analysis performed using the ITSG Caron et al., 2018 GRACE ocean and SLBC_cci v2 steric component. If we consider full years for the trend estimation, i.e., between August 2003 (instead of Jan. 2003) and August 2016, the residual trend slightly decreases to 0.27±0.36 mm/yr with a RMS of 2.7 mm. The steric + GRACE and the residual trend uncertainties are estimated as the root square sum (RSS) of the steric and GRACE uncertainties.

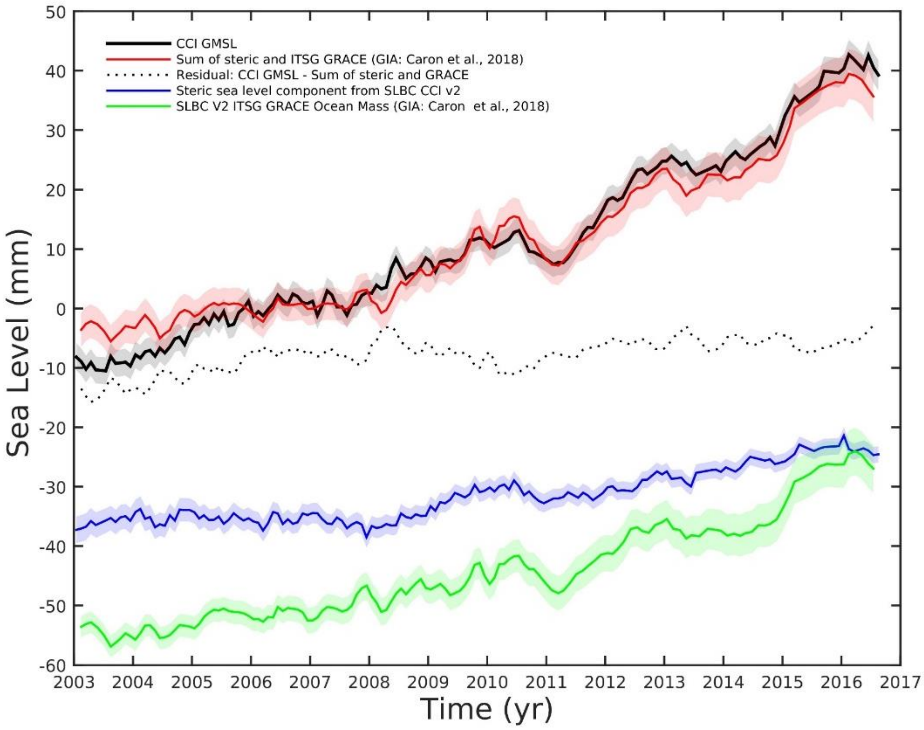

Figure 3.11: Sea level budget analysis using ITSG Caron et al., 2018 GRACE (green) ocean mass and SLBC_cci v2 steric component (blue). The observed GMSL is in black, sum of GRACE and steric in red and residual time series in black dotted lines.

3.3 Discussion and Conclusions

In terms of trend estimation, SLBC_cci v2 products have brought the global sea level budget mis-closure over P(1) closer to zero, as compared to the v1 products. The inclusion of peripheral glaciers in Greenland has contributed to this improvement. For 1993-2016, the residual trend and the RMS of the residuals amount to 0.14±0.3 mm/yr and 2.2 mm, respectively. For 2003-2016, the residual trend amounts to 0.17±0.3 mm/yr and 0.33±0.36 mm/yr using the sum of mass components and GRACE ocean mass respectively.

Over 2003-2016, the sea level budget residual time series are well within the uncertainty estimates contributed by all sea level components. Figure 3.12 displays the sea level budget residual time series estimated using (a) sum of all v2 components with AIS and GIS based on radar altimetry, (b) sum of v2 components with AIS and GIS from GRACE, (c) sum of steric and GRACE ocean mass. The corresponding uncertainties are also displayed. The residual uncertainties are estimated as the root square sum (RSS) of the GMSL and sea level components uncertainties. We can observe that the residual budget time series are well within their uncertainty range.

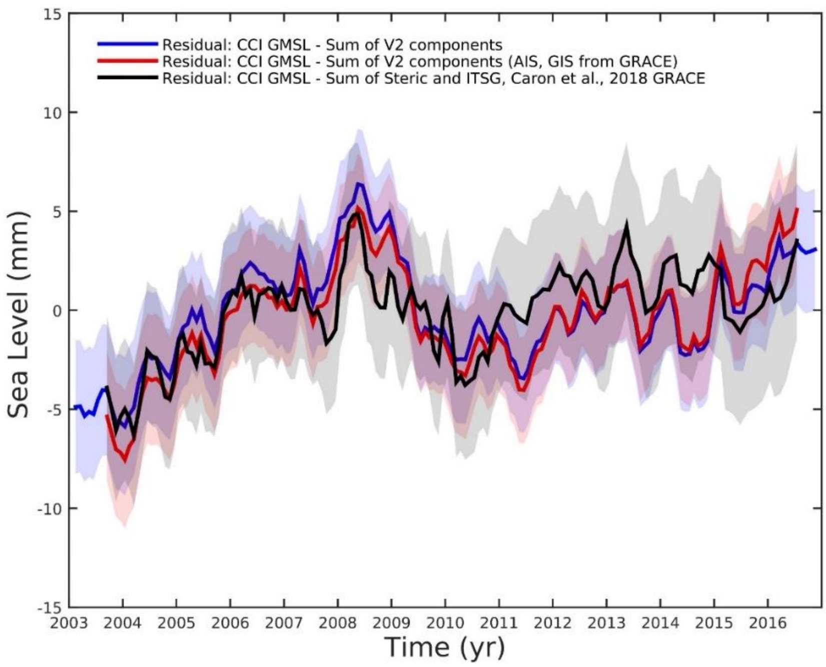

Figure 3.12: Sea level budget residual time series estimated using (a) sum of all v2 components with AIS and GIS based on radar altimetry (in blue), (b) sum of v2 components with AIS and GIS from GRACE (in red), (c) sum of steric and GRACE ocean mass (in black)

In terms of interannual variability, important sea level budget residuals still remain between 2003 and 2011 and have been attributed to steric and land water components. Efforts are needed to understand the cause of their roles in the sea level budget mis-closure in terms of interannual variability in the future.

4 Arctic Sea Level Change

Sea level change, an important indicator of climate change, integrates the response of several components of the earth's system (ocean, atmosphere, cryosphere and hydrosphere) to natural and anthropogenic forcing. Studies of the sea level budget helps us to quantify sea level changes and its causes. In turn, this yields better understanding of dominant processes and temporal changes (e.g., acceleration) of individual components. An aim of the CCI Sea Level Budget Closure project is to use the CCI data products, together with other data sources to re-assess the sea-level budget of the Arctic Ocean. Note that the specific focus on the Arctic sea level budget is due to the fact that the region has warmed at a rate about twice the rest of the globe during the recent decades. The sea level of the region may therefore be influenced by the oceanic thermal expansion, as well as the melting of the high latitude glaciers and the Greenland ice sheets associated with the warming of the Arctic region in recent decades.

4.1 Data update

The DTU Arctic altimeter data. The spatial distribution of data coverage of the altimeter data in the Arctic Ocean is shown in Figure 4.1. It is clear that distinct areas inside the Arctic Ocean only have data availability less than 25%. As this is also seasonally dependent it can be concluded that large part of the Arctic Ocean offers limited altimeter-based estimates of sea surface height (SSH), in particular during winter. In turn, the time series and associated trends of altimeter-based SSH estimates are inflicted with uncertainties.

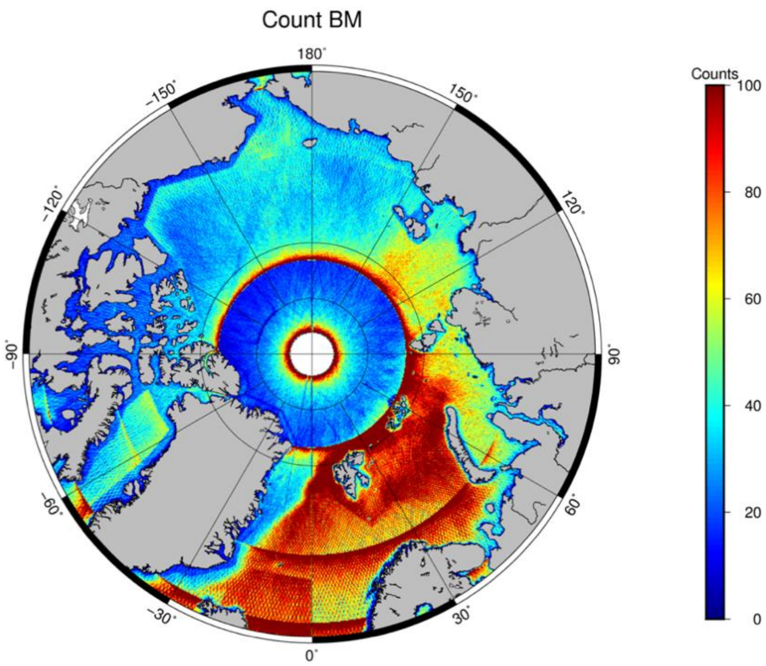

Figure 4.1: Illustration of the altimeter-based data coverage for the Arctic Ocean for the year 2015.

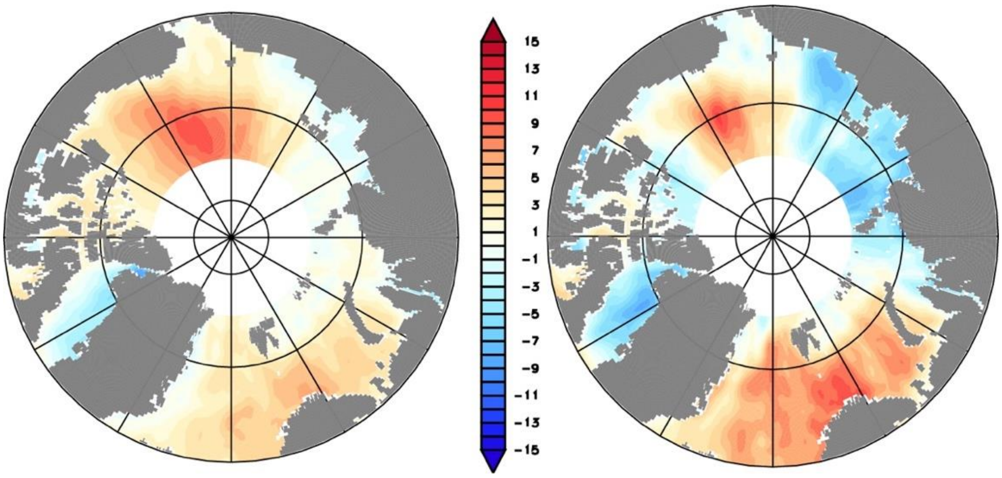

Figure 4.2: Sea level trend for the two time periods: 1993-2016 (left; mean **2.4 mm/yr**) and 2003-2016 (right; mean **1.2 mm/yr**)

A reduction in the overall trend in the Arctic sea level is noted during the past 14 years (2003-2016; 1.2 mm/yr) compared to the full time period (1993-2016; 2.4 mm/yr), see Figure 4.2. There is also a distinct evidence of sea level decline on the Siberian shelf during the latter period.

GRACE Ocean mass data: SH solution and mascons are the two main solutions of GRACE ocean mass data. Examples of 3 SH-Solutions estimated in the SLB_cci project is shown in Figure 4.3. The SH solutions cannot include areas close to the coast (~300km), as they would include signal that leaks in from the continents. Hence, the total spatial coverage in the Arctic is rather poor, leading to non-preferred SH solutions in the Arctic Ocean.

In contrast, the mascons are not just representing gravity measurements, they also include localised pre-assumptions and a-priori information. In this project, two mascons products, one from JPL and one from GSFC, for the period 2003-2016 are used to examine the ocean mass change in the Arctic Ocean (Figure 4.4).

Our analysis reveals that the trend in ocean mass change for the time period 2003-2016 (Figure 4.4) is much higher in the GSFC mascon product (4.9 mm/yr) compared to the JPL data (2.0 mm/yr).

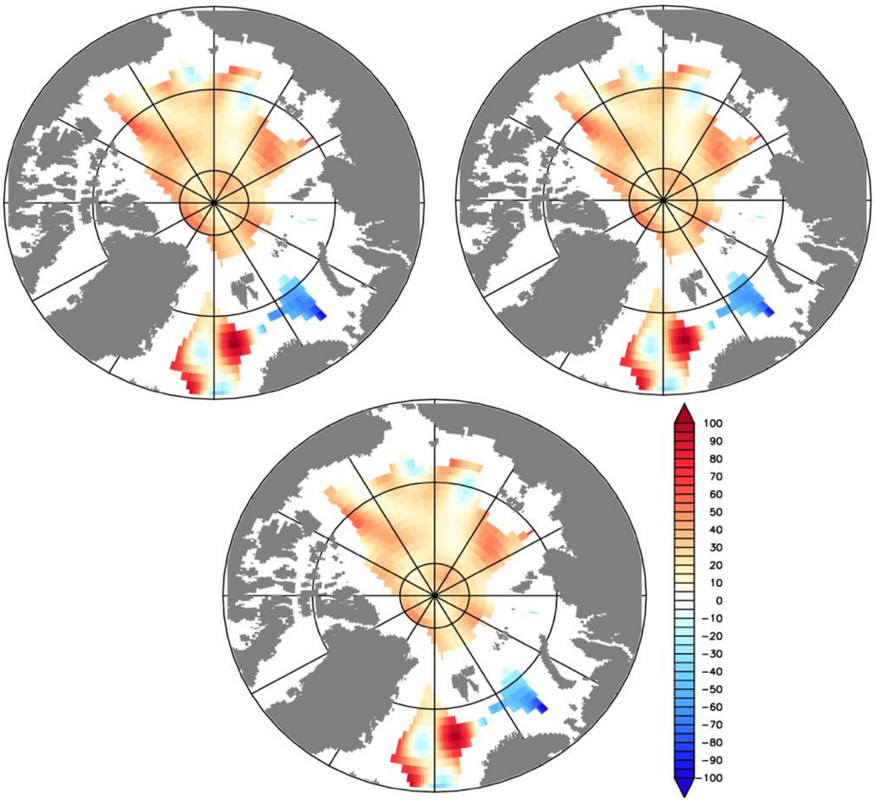

Figure 4.3: Ocean mass change gridded products (April 2011; kg/m²) based on ITSG2018 using three different GIA models, A2013-Ice5Gv2 (upper left), Ice-6Gv5a (upper right), CaronIvins2018 (lower)

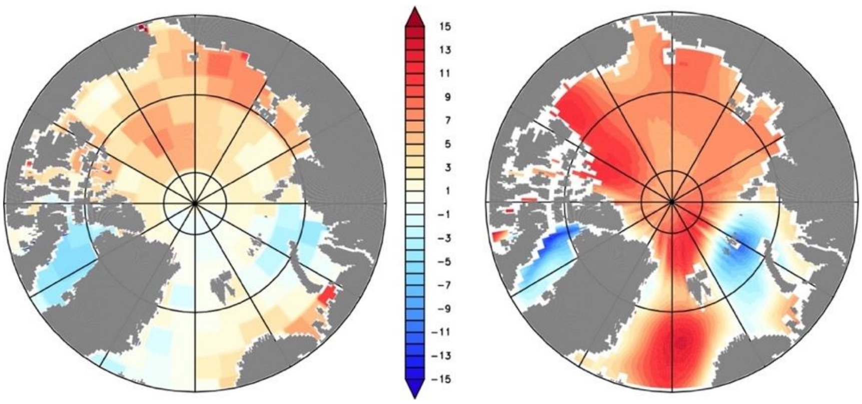

Figure 4.4: Trend in ocean mass change for the time period 1993-2016: (left) JPL (mean **2.0 mm/yr**); (right) GSFC (mean **4.9 mm/yr**)

Additional datasets used for the sea level budget assessment include:

- **EN4,** version 4 of the Met Office Hadley Centre "EN" series of global quality-controlled ocean temperature and salinity profiles (T&S) for the time period 2003-2016.
- Monthly gridded **NERSC TOPAZ4** reanalyses data for the period 2003-2016.

4.2 Budget Assessment

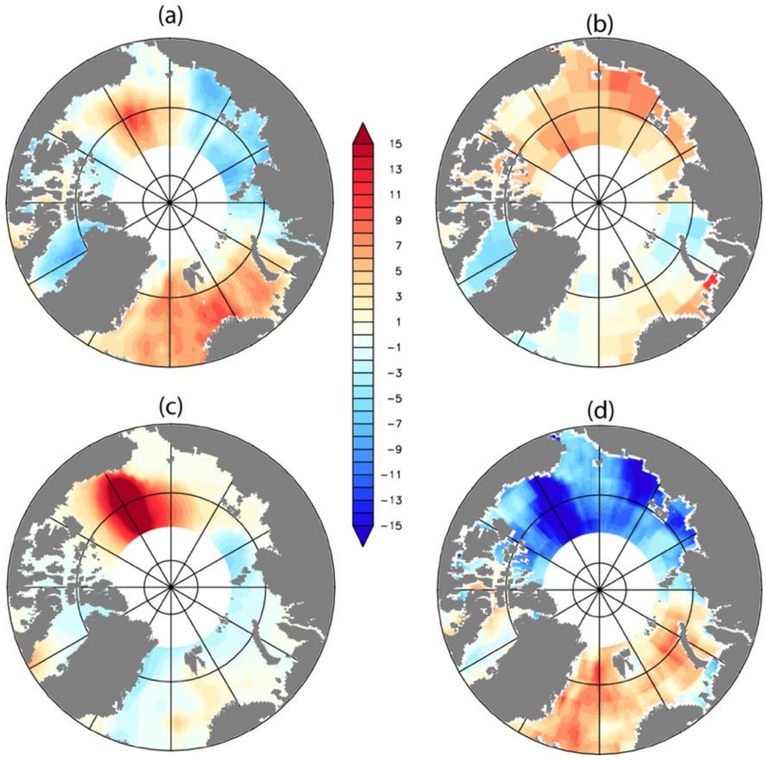

Figure 4.5: Trend in (a) sea level; mean **1.2 mm/yr**, (b) ocean mass change; mean **2.0 mm/yr**, and (c) steric height; mean **1.4 mm/yr** for the time period 1993-2016. (d) The residual trend (ssh-ocean mass+steric); mean **-2.2 mm/yr**.

The Arctic sea level budget from observations is shown in Figure 4.5. In this assessment the coverage for the Arctic region is the entire ocean area north of 65°N. The sum of the ocean mass change (mean 2.0 mm/yr) and steric height (mean 1.4 mm/yr) trend in the Arctic Ocean is found to be higher than the trend in Arctic Sea level (mean 1.2 mm/yr). The residual is found to be bipolar, being positive in the Nordic Seas- Barents Sea region and negative over the rest of the Arctic, especially in the Beaufort Gyre and in parts of the Siberian Shelf. A positive signature in the residual indicates that the trend in sea level is higher compared to the sum of the trend in ocean mass change and steric height.

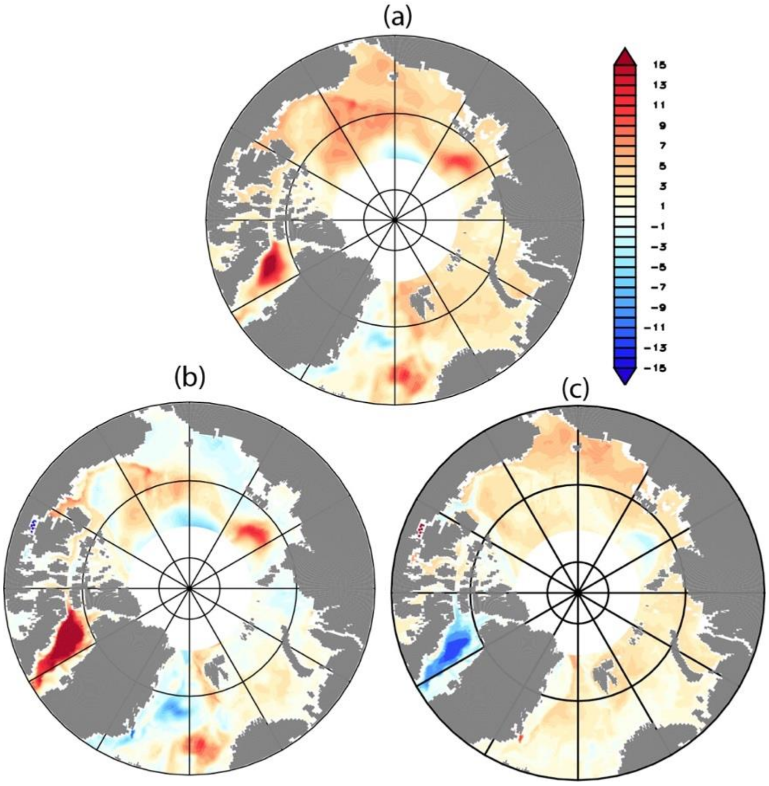

Figure 4.6: Trend in TOPAZ sea level (**3.5 mm/yr**), steric height (**2.0 mm/yr**) and ocean mass change (**1.5 mm/yr**) for the time period 1993-2016.

The TOPAZ sea level budget assessment is shown in Figure 4.6 and is compared to the observation-based budget assessment of the same quantities shown in Figure 4.5. The total ssh trend is clearly different being almost 3-times larger in the TOPAZ4 simulations (mean 3.5 mm/yr) compared to the altimeter-based observations (mean 1.2 mm/yr). The steric components, on the other hand, are comparable (mean 2.0 mm/yr for TOPAZ4 versus mean 1.4 mm/yr for EN4). This is somewhat expected as TOPAZ4 is assimilating the EN4 data set. However, several distinct regional differences are noticed, such as in the Beaufort Gyre and the Lofoten Basin within the Norwegian Sea. Note that the trends in the mass change components are not comparable at all. First, the TOPAZ4 value is simply emerging from the total SSH minus the steric component and is not properly accounting for the ice sheet melting and change of the geoid. Second, the GRACE values are representing one of the two mascon products, none of which have been adequately validated for the high latitude and Arctic Ocean.

4.3 Discussion and Conclusions

The sea level trend in the high latitude seas and Arctic Ocean (Figure 4.5a) shows that there are two distinct regions with increasing trend (Nordic Seas-Barents Sea and Beaufort Sea) and two regions with decreasing trend (Canadian Archipelago and Siberian Shelf) in sea level. This is an indication of the complexity of the Arctic region, where distinct local differences are prominent due to the presence of sea ice as well as the large range in water depths.

In order to further assess these results, the time series and corresponding mean linear trend estimates are compared in Figure 4.7. This comparison includes the SSH from altimetry, the mass changes derived from GRACE and the ocean steric contribution derived from the EN4 in-situ climatology of temperature and salinity.

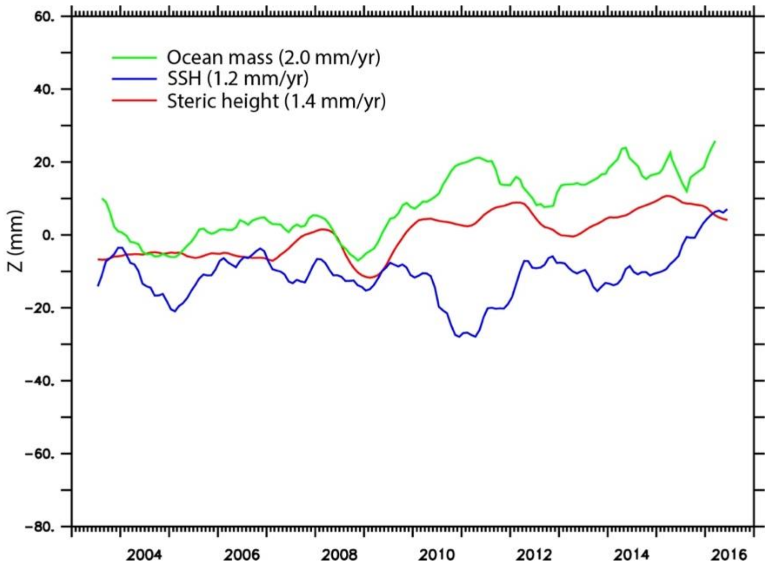

Figure 4.7: Time series (1 year running mean) and corresponding mean linear trend estimates (in parenthesis) of the sea surface height (SSH) from altimetry (blue), mass changes from ice sheet melting converted to ssh from GRACE (green), and ocean steric contribution (red) for the time period 2003 to 2016. Area corresponds to the entire Arctic region outside the polar gap.

Inter-comparison of the time series of the sea level change and ocean mass change over the Arctic region reveals two distinct time periods during which the two time-series are either in-phase or out-of-phase. During the 7-year time-period (2003-2009) the time series are in-phase, while during the next 6 years, 2010-2015, they are out-of-phase. Moreover, the steric height variability is in phase with the ocean mass change over the entire time period. This result is yet another example of the complexity and challenges associated with the sea level budget study of the high latitude seas and Arctic Ocean.

All in all, these results suggest that:

- It is highly necessary to:
    - Improve the geographical and seasonal altimeter coverage and reduce polar gap;
    - Improve estimation of the steric component through more in-situ observations with better coverage;
    - Create long timeseries from multiple altimeter satellites whereby biases connected with different corrections and processing methods are reliably removed;

- Closing of the regional sea level budget for the Arctic Ocean and neighboring seas at (seasonal) and annual time scale will depend on reliable estimates with uncertainties of the individual components, notably:
    - proper estimates of seasonal bias in data coverage, especially wrt. sea ice;
    - better estimate of leakage of signals in the GRACE data due to coarse spatial resolutions;
    - including trend assessment for sub-regions, in addition to the entire region north of 66^{o}N.

- Future perspectives include:
    - Correction of LRM altimeter data (e.g., water level from sea ice covered oceans) using ALES+ ocean re-tracker;
    - A new Global tailored-kernel solution (similar to mascons) of the GRACE ocean mass data based on SH.
    - Assimilation of SMOS salinity in TOPAZ model (an initiative funded by ESA under the Arctic + Salinity project).
    - Doubling the resolution of the TOPAZ model (funded by the Copernicus Marine Services).

5 References

A, G., Wahr, J., and Zhong, S. (2013): Computations of the viscoelastic response of a 3-D compressible Earth to surface loading: an application to Glacial Isostatic Adjustment in Antarctica and Canada. *Geophysical Journal International*, 192(2), 557-572. doi: 10.1093/gji/ggs030.

Ablain M, Meyssignac B, Zawadzki L, Jugier R, Ribes A, Cazenave A, Picot N (2019, *in review*): Uncertainty in Satellite estimate of Global Mean Sea Level changes, trend and acceleration, *Earth Syst. Sci. Data Discuss*., https://doi.org/10.5194/essd-2019-10

Ablain M., R. Jugier, L. Zawadki, and N. Taburet (2017): *The TOPEX-A Drift and Impacts on GMSL Time Series*. AVISO Website. October 2017. https://meetings.aviso.altimetry.fr/fileadmin/user_upload/tx_ausyclsseminar/files/Poster_OSTST17_GMSL_Drift_TOPEX-A.pdf.

Chambers, D. P., and J. A. Bonin (2012): Evaluation of Release-05 GRACE time-variable gravity coefficients over the ocean, *Ocean Sci*., 8, 859–868, doi: 10.5194/os-8–859-2012.

Caron, L., Ivins, E. R., Larour, E., Adhikari, S., Nilsson, J., and Blewitt, G. (2018): GIA model statistics for GRACE hydrology, cryosphere, and ocean science. *Geophysical Research Letters*, 45, 2203–2212. doi: 10.1002/2017GL076644.

Dieng, H. B., Cazenave, A., von Schuckmann, K., Ablain, M., & Meyssignac, B. (2015). Sea level budget over 2005-2013: missing contributions and data errors. Ocean Science, 11(5).

Dieng, H.B, A. Cazenave, B. Meyssignac, and M. Ablain (2017): New estimate of the current rate of sea level rise from a sea level budget approach, *Geophysical Research Letters*, 44, doi:10.1002/2017GL073308.

Good, S. A., M. J. Martin, and N. A. Rayner (2013): EN4: Quality controlled ocean temperature and salinity profiles and monthly objective analyses with uncertainty estimates, *J. Geophys. Res. Oceans*, 118, 6704–6716, doi:10.1002/2013JC009067.

Groh, A.; Horwath, M.; Gutknecht, B.D.; Hogg, A.; Shepherd, A. (2019): Improved estimates of Antarctic mass balance from updated GRACE solution series. Poster presented at ESA Living Planet Symposium 2019, Milano

Horwath, M., and Groh, A. (2016): The GRACE mass change estimators developed for ESA's CCI ice sheet mass balance products. *Proc. GRACE Science Team Meeting 2016*, Potsdam, 5-7 November 2016. http://www.gfz-potsdam.de/en/section/global-geomonitoring-and-gravity-field/topics/development-operation-and-analysis-of-gravity-field-satellite-missions/grace/gstm/gstm-2016/proceedings/.

Horwath, M.; Novotny, K.; Cazenave, A.; Palanisamy, H.; Marzeion, B.; Paul, F.; Döll, P.; Cáceres, D.; Hogg, A.; Shepherd, A.; Otosaka, I.; Forsberg, R.; Barletta, V.R.; Simonsen, S.; Andersen, O.B.; Rose, S.K.;Ranndal, H.; Johannessen, J.A.; Raj, R.P.; Gutknecht, B.D.; Merchant, Ch.J.; von Schuckmann, K.: *ESA Climate Change Initiative (CCI) Sea Level Budget Closure (SLBC_cci). Product Description Document D2.4.2: Version 2 data sets and uncertainty assessments*. Version 1.2, 18 Jun. 2019.

Ishii, M., & Kimoto, M. (2009). Reevaluation of historical ocean heat content variations with time-varying XBT and MBT depth bias corrections. Journal of Oceanography, 65(3), 287-299.

Johnson, G. C., and D. P. Chambers (2013): Ocean bottom pressure seasonal cycles and decadal trends from GRACE Release-05: Ocean circulation implications, *J. Geophys. Res. Oceans*, 118, 4228–4240, doi: 10.1002/jgrc.20307.

Klinger, B., Mayer-Gürr, T., Behzadpour, S., Ellmer, M., Kvas, A., and Zehentner, N. (2016): The new ITSG-Grace2016 release. *Geophys. Res. Abstr*., 18, EGU2016–11547.

Levitus S., et al. (2012): World ocean heat content and thermosteric sea level change (0–2000 m), 1955–2010. *Geophys. Res. Lett.*, 39, L10603. doi: 10.1029/2012GL051106.

Luthcke, S. B., Sabaka, T. J., Loomis, B. D., Arendt, A. A., McCarthy, J. J., and Camp, J. (2013): Antarctica, Greenland and Gulf of Alaska land-ice evolution from an iterated GRACE global mascon solution. *J. Glac.,* 59(216), 613–631. doi: 10.3189/2013JoG12J147.

Marzeion, B., Jarosch, A. H., and Hofer, M. (2012): Past and future sealevel change from the surface mass balance of glaciers, *The Cryosphere*, 6, 1295–1322, doi: 10.5194/tc-6-1295-2012.

Mayer-Gürr, T., Behzadpour, S., Ellmer, M., Klinger, B., Kvas, A., Strasser, S., & Zehentner, N. (2018a). ITSG-Grace2018: The new GRACE time series from TU Graz. *Abstract from GRACE / GRACE-FO Science Team Meeting 2018*, Potsdam, Germany.

Mayer-Gürr, T., Behzadpour, S., Ellmer, M., Kvas, A., Klinger, B., and Zehentner, N. (2016): ITSG-Grace2016 - Monthly and Daily Gravity Field Solutions from GRACE. *GFZ Data Services*. doi: 10.5880/icgem.2016.007.

Mayer-Gürr, Torsten; Behzadpur, Saniya; Ellmer, Matthias; Kvas, Andreas; Klinger, Beate; Strasser, Sebastian; Zehentner, Norbert (2018b): ITSG-Grace2018 - Monthly, Daily and Static Gravity Field Solutions from GRACE. *GFZ Data Services*. *http://doi.org/10.5880/ICGEM.2018.003*

Nagler, T., et al., (2017). Comprehensive Error Characterisation Report (CECR). Antarctic_Ice_Sheet_cci project, ESA's Climate Change Initiative, version 3.0, 01 November 2017. Available from: http://www.esa-icesheets-antarctica-cci.org/

Peltier W.R. (2004): Global glacial isostasy and the surface of the ice-age Earth: the ICE-5G (VM2) model and GRACE, *Annual Review of Earth and Planetary Sciences* 32:111.

Peltier, W. R., Argus, D. F., and Drummond, R. (2015): Space geodesy constrains ice age terminal deglaciation: The global ICE-6G_C (VM5a) model: Global Glacial Isostatic Adjustment. *J. Geophys. Res. Solid Earth*, 120(1), 450–487. doi: 10.1002/2014JB011176.

Purkey, S. and Johnson, G. C.: Warming of global abyssal and deep southern ocean waters between the 1990s and 2000s: Contributions to global heat and sea level rise budget, J. Climate, 23, 6336–6351, https://doi.org/10.1175/2010JCLI3682.1, 2010.

Schröder, L., Horwath, M., Dietrich, R., Helm, V., Broeke, M. R., & Ligtenberg, S. R. (2019). Four decades of Antarctic surface elevation changes from multi-mission satellite altimetry. The Cryosphere, 13(2), 427-449.

Shepherd, A., Ivins, E., Rignot, E., Smith, B., van den Broeke, M., Velicogna, I., ..., Groh, A., ..., Horwath, M, ..., Schröder, L., et al. (2018). Mass balance of the Antarctic Ice Sheet from 1992 to 2017. Nature, 556, pages 219-222.

Uebbing, B, Kusche, J., Rietbroek, R., Landerer, F.W. (2018): Processing choices affect ocean mass estimates from GRACE JGR Oceans https://doi.org/10.1029/2018JC014341

von Schuckmann K, and Le Traon P-Y (2011): How well can we derive Global Ocean Indicators from Argo data? *Ocean Sci.,* 7:783-791, doi: 10.5194/os-7-783-2011.

WCRP Global Sea Level Budget Group (the) (2018): Global sea level budget, 1993-present, *Earth System Science Data*, 10, 1551-1590, doi: 10.5194/essd-10-1551-2018.

WGMS (2016): *Fluctuations of Glaciers Database*. World Glacier Monitoring Service, Zurich, Switzerland. doi: 10.5904/wgms-fog-2016-08.